nature methods

BRIEF COMMUNICATION

https://doi.org/10.1038/s41592-018-0238-1

Imaging cellular ultrastructures using expansion microscopy (U-ExM)

Davide Gambarotto[1,9], Fabian U. Zwettler[2,9], Maeva Le Guennec[1], Marketa Schmidt-Cernohorska[1,7], Denis Fortun[3,8], Susanne Borgers[1], Jörn Heine[4], Jan-Gero Schloetel[4], Matthias Reuss[4], Michael Unser[5], Edward S. Boyden[6], Markus Sauer[2]*, Virginie Hamel[1]* and Paul Guichard[1]*

Determining the structure and composition of macromolecular assemblies is a major challenge in biology. Here we describe ultrastructure expansion microscopy (U-ExM), an extension of expansion microscopy that allows the visualization of preserved ultrastructures by optical microscopy. This method allows for near-native expansion of diverse structures in vitro and in cells; when combined with super-resolution microscopy, it unveiled details of ultrastructural organization, such as centriolar chirality, that could otherwise be observed only by electron microscopy.

Cells comprise organelles, large macromolecular assemblies displaying specific structures that for decades could be visualized only by electron microscopy[1]. Although super-resolution fluorescence microscopy has evolved as a very powerful method for subdiffraction-resolution fluorescence imaging of cells, the visualization of ultrastructural details of macromolecular assemblies remains challenging[2].

Recently an innovative method called expansion microscopy (ExM) emerged in which immunolabeled samples are physically expanded, and thus can undergo super-resolution imaging by standard fluorescence microscopy[3,4] (Supplementary Fig. 1a). Alternative ExM protocols such as protein-retention ExM[5] and magnified analysis of the proteome (MAP)[6] have been developed that cross-link proteins in the polymer matrix and allow for post-expansion immunostaining (Supplementary Fig. 1a). However, it remains unclear whether these methods preserve the molecular architecture of organelles.

Here we first set out to characterize the macromolecular-expansion performance of established ExM and MAP protocols[4,6]. As reference structures, we used isolated *Chlamydomonas* centrioles, which have a characteristic ninefold microtubule triplet-based symmetry, forming a polarized cylinder ~500 nm long and ~220 nm wide[7] (Supplementary Fig. 1b). We immunolabeled isolated centrioles for α-tubulin, to visualize the centriolar microtubule wall, and for polyglutamylated tubulin (PolyE) present only on the central region of the centriole[7,8]. Although the cylindrical nature of the centriole was visible with the PolyE signal in confocal microscopy, it was impossible to visualize the canonical ninefold symmetry of the microtubule triplets (Fig. 1a). Moreover, we noticed antibody competition when we costained for both α-tubulin and PolyE, with both antibodies recognizing epitopes on the C-terminal moiety of tubulin.

Next, we expanded centrioles with both ExM and MAP protocols and imaged the samples by confocal microscopy followed by HyVolution (Fig. 1b,c). The gels expanded ~4.2-fold (ExM) and ~3.5-fold (MAP). We noticed that the diameter of the centriole in ExM-expanded samples was markedly larger than expected from the determined expansion factor. Indeed, the PolyE signal showed a 1.4× enlargement with an average centriole diameter of 308 ± 42 nm after expansion, compared with the diameter of 216 ± 17 nm determined from non-expanded centrioles imaged by direct stochastic optical reconstruction microscopy (dSTORM)[9] (Fig. 1e, Supplementary Figs. 1c and 2, and Methods), suggesting an anisotropic macromolecular expansion. Moreover, the tubulin signal appeared inhomogeneous, probably because of epitope masking of antibodies to PolyE (Fig. 1b (lateral view) and Supplementary Fig. 3a,b). However, we noticed that the ninefold symmetry of centrioles could be visualized, albeit not perfectly, in ExM-treated centrioles (Fig. 1b, Supplementary Fig. 3c,d). In contrast, we observed that the MAP-treated centrioles appeared 1.6 times smaller, with an average diameter of 133 ± 27 nm (Fig. 1c,e), again suggesting inhomogeneous macromolecular expansion. As a consequence, the ninefold symmetry of the PolyE-labeled samples was not apparent (Fig. 1c, Supplementary Fig. 3e). However, we observed a reduction in antibody competition (Fig. 1c).

On the basis of these results, we set out to develop a new method of ExM that could preserve the overall ultrastructure of isolated organelles. Capitalizing on the MAP protocol[6], we found that avoiding fixation and using a combination of low concentrations of formaldehyde (FA; 0.3–1%) and acrylamide (AA; 0.15–1%) resulted in intact centriolar expansion with correct diameters (Supplementary Fig. 3f–h). Therefore, we termed the approach ultrastructure expansion microscopy (U-ExM). Application of U-ExM to isolated centrioles revealed unambiguously the ninefold symmetry of the centriole with both α-tubulin and PolyE signal, with correct diameters of 195 ± 12 nm and 225 ± 15 nm, respectively (Fig. 1d,e). U-ExM centrioles showed good overall preservation of the centriolar shape compared with that in cryo-electron microscopy (cryo-EM) images (Supplementary Fig. 4a,b), as well as perfect isotropic expansion of centrioles compared with that achieved by other methods (Fig. 1f). Moreover, we were able to alleviate the antibody competition, as demonstrated by central core decoration of the PolyE signal with retention of complete tubulin decoration of the centriolar wall

[1]Department of Cell Biology, Sciences III, University of Geneva, Geneva, Switzerland. [2]Department of Biotechnology and Biophysics, Biocenter, University of Würzburg, Würzburg, Germany. [3]Signal Processing Core of Center for Biomedical Imaging (CIBM-SP), EPFL, Lausanne, Switzerland. [4]Abberior Instruments GmbH, Göttingen, Germany. [5]Ecole Polytechnique Fédérale de Lausanne (EPFL), Biomedical Imaging Group, Lausanne, Switzerland. [6]Massachusetts Institute of Technology (MIT), Cambridge, MA, USA. [7]Present address: Laboratory of Adaptative Immunity, Institute of Molecular Genetics, Academy of Sciences of the Czech Republic, Prague, Czech Republic. [8]Present address: ICube, CNRS, University of Strasbourg, Illkirch, France. [9]These authors contributed equally: Davide Gambarotto, Fabian U. Zwettler. *e-mail: m.sauer@uni-wuerzburg.de; virginie.hamel@unige.ch; paul.guichard@unige.ch

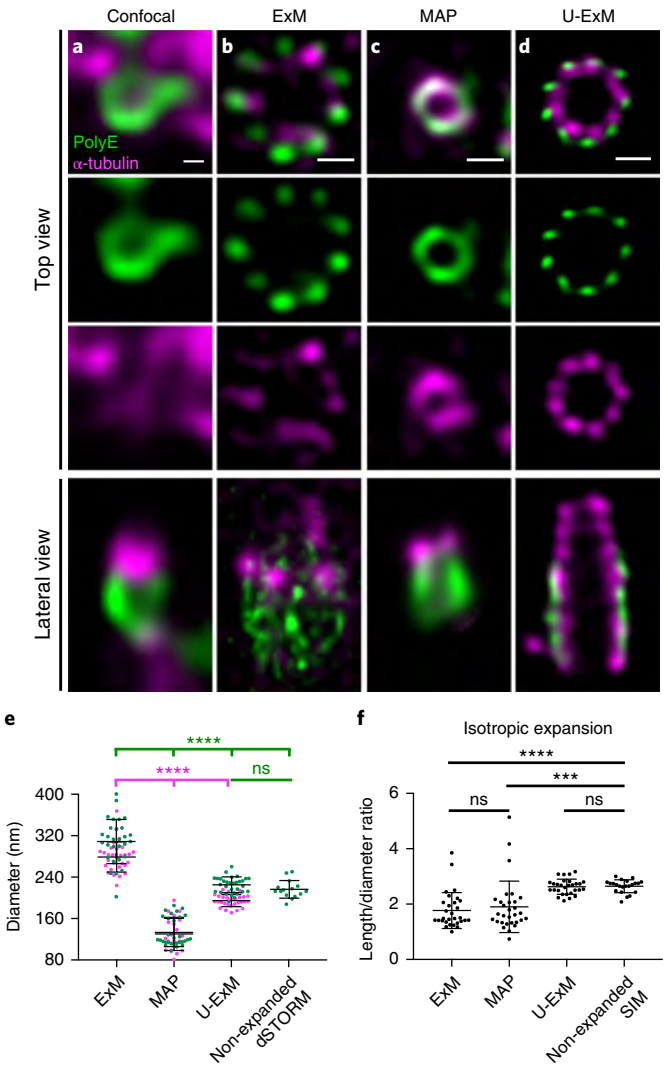

Fig. 1 | Centriole expansion with U-ExM. a–d, Non-expanded (**a**) and expanded (**b–d**) isolated centrioles stained for PolyE (green; Alexa Fluor 488) and α-tubulin (magenta; Alexa Fluor 568) and imaged by confocal microscopy followed by HyVolution. Centrioles were expanded by ExM (**b**), MAP (**c**), or U-ExM (**d**). Scale bars, 100 nm (**a**) or 450 nm (**b**,**c**,**d**). Representative images from 2 (**a**) or 3 (**b**,**c**,**d**) independent experiments are shown. **e**, Diameter of the centrioles in the different conditions. Green and magenta dots represent PolyE and α-tubulin diameters, respectively. Averages and s.d. are as follows. PolyE: 308 ± 42 nm, 133 ± 27 nm, 225 ± 15 nm, and 216 ± 17 nm for ExM, MAP, U-ExM, and non-expanded dSTORM, respectively. $n = 30$ centrioles for each condition (data from 3 independent experiments) except dSTORM, where $n = 15$ non-expanded centrioles (1 experiment). α-tubulin: 279 ± 29 nm, 130 ± 32 nm, and 195 ± 12 nm for ExM ($n = 29$ centrioles), MAP ($n = 20$ centrioles), and U-ExM ($n = 29$ centrioles), respectively. Data from 3 independent experiments. Statistical significance was assessed by one-way ANOVA: $^{****}P < 0.0001$, ns (nonsignificant) = 0.77. **f**, Isotropic expansion measured as the ratio between the centriole length and diameter. Average ratios and s.d. are as follows: ExM, 1.8 ± 0.6 ($n = 30$ centrioles); MAP, 1.9 ± 0.9 ($n = 30$ centrioles); U-ExM, 2.6 ± 0.3 ($n = 29$ centrioles); non-expanded structured illumination microscopy (SIM), 2.6 ± 0.2 ($n = 22$ centrioles). Data from 3 independent experiments except for SIM, where they are from a single experiment. Statistical significance was assessed by one-way ANOVA: $^{****}P < 0.0001$; $^{***}P = 0.0002$; ns (non-significant) = 0.84 for ExM versus MAP and 0.99 for U-ExM versus non-expanded SIM.

(Fig. 1d, lateral view). Finally, we found that the ninefold symmetry was clearly visible and the centriolar roundness was best preserved with U-ExM compared with the results of other ExM protocols (Supplementary Fig. 4c,d).

We then sought to test the potential of U-ExM by comparing confocal images of expanded procentrioles and nonexpanded centrioles imaged by dSTORM, both stained for PolyE (Supplementary Fig. 5a–e and Fig. 2a–c). Here the ninefold-symmetric microtubule triplets could not be visualized unambiguously by dSTORM, unlike with confocal imaging before and after deconvolution of U-ExM-expanded samples (Fig. 2a–c, Supplementary Fig. 5f–h). Overall, U-ExM combined with confocal microscopy showed higher labeling efficiency than in unexpanded dSTORM images and apparent spatial resolution (Supplementary Fig. 5i–k), allowing the characterization of ultrastructural components of macromolecular assemblies.

We next set out to analyze precisely PolyE localization on the microtubule triplets with U-ExM (Supplementary Fig. 6 and 7). U-ExM revealed that PolyE covered the outer surface of the tubulin signal with nine discrete puncta at both proximal and distal ends (Supplementary Fig. 6a and Supplementary Videos 1 and 2). To prevent any artifact due to the anisotropic resolution of confocal microscopy, we next carried out an isotropic 3D reconstruction using a recent 'reference-free' reconstruction approach[10] (Methods) (Supplementary Fig. 6b–f). This result confirmed PolyE localization with nine clear, discrete signals at both distal and proximal ends. By measuring the diameters of both PolyE and α-tubulin signals, we found that PolyE had a measured expanded diameter 88–140 nm larger than that of tubulin (Supplementary Fig. 6g–i). By modeling several PolyE localizations on each microtubule triplet, we found that PolyE localized on the C-microtubule; this established that U-ExM is able to distinguish a C-microtubule triplet localization for polyglutamylated tubulin in mature centrioles (Supplementary Fig. 7).

To further investigate the ability of U-ExM to reveal the molecular architecture of centrioles, we combined it with stimulated emission depletion (STED) microscopy using either single-color (Fig. 2d) or dual-color imaging (Supplementary Fig. 8a,b, and Supplementary Video 3). As shown by electron microscopy, centrioles are composed of nine microtubule triplets with a characteristic angle arranged in a clockwise manner as seen from the proximal side (Supplementary Fig. 8c). Notably, U-ExM-treated centriole pairs imaged with DyMIN[11] gave us a glimpse of the triplet structure of microtubules on the procentrioles (Supplementary Fig. 8d), as well as visualization of the anticlockwise and clockwise orientations of microtubule triplets in procentrioles (Fig. 2d). In some cases, we could even identify three distinct fluorescent peaks for microtubule triplets that possibly corresponded to the A-, B-, and C-microtubules (Fig. 2d, arrowhead). Furthermore, we found a similar microtubule triplet angle of ~120° in electron microscopy and U-ExM images (Fig. 2e), thus corroborating that U-ExM preserved the nanometric conformation of the sample.

Next we tested whether U-ExM can be applied in cellulo. We first expanded unfixed CW15$^-$ *Chlamydomonas reinhardtii* cells. Although we observed a slight increase in centriole diameter in cellulo (236 ± 18 nm for PolyE and 212 ± 22 nm for tubulin), we were able to confirm correct isotropic expansion and ninefold symmetry (Supplementary Fig. 9a–d). In addition, we found that U-ExM allowed visualization of the ninefold symmetry of the axoneme with a tubulin diameter of 192 nm, in agreement with a previous description[12] (Supplementary Fig. 10 and Supplementary Video 4). Moreover, we found that the nine microtubule doublets were highly polyglutamylated, whereas the central pair was only weakly polyglutamylated (Supplementary Figs. 10a and 11a–f). By modeling different polyglutamylation localizations on the axoneme, we found that polyglutamylation marks were deposited on the surface of the

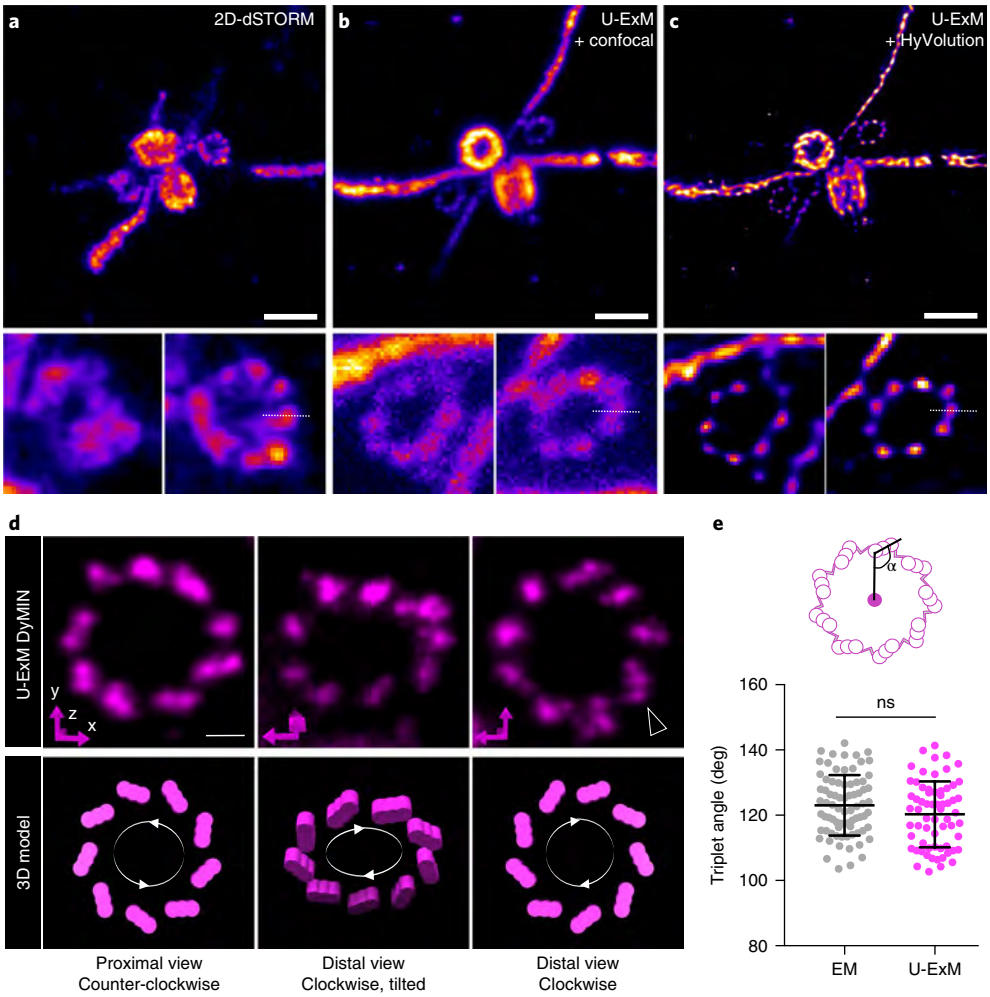

Fig. 2 | U-ExM reaches dSTORM precision limits. a, Top, 2D dSTORM image of an isolated centriole. Scale bar, 250 nm. **b**, Top, Confocal image of a centriole expanded with U-ExM (0.7% FA + 1% AA). **c**, Top, Deconvoluted image of the centriole in **b** obtained with HyVolution. **b**,**c**, Scale bar, 1 µm. **a**–**c**, Bottom, magnified (3× relative to primary images) views of the procentrioles shown in the respective image above. The dotted white lines correspond to the plot line profile used to calculate the FWHM shown in Supplementary Fig. 5i–k. Representative images from 1 (**a**) or 3 (**b**,**c**) independent experiments. **d**, Top, representative DyMIN images of procentrioles stained for α-tubulin (magenta; STAR RED), highlighting their counter-clockwise or clockwise orientations. Bottom, the interpretation of such orientations in a 3D schematic model. Arrowhead points to individual blades within a microtubule triplet (11 out of 90 procentrioles). Scale bar, 200 nm. Representative images from 2 independent experiments. **e**, Quantification of the angle between the center of the centriole and the microtubule triplet both from electron microscopy (123° ± 9°, average ± s.e.) ($n = 77$ triplets) and DyMIN (120° ± 10°) ($n = 65$ triplets) images. $P = 0.0912$, unpaired two-tailed t-test.

B-tubule facing the flagellar lumen of *Chlamydomonas* axonemes, as previously proposed for both *Chlamydomonas* and *Tetrahymena*[13–16] (Supplementary Fig. 11g–q).

We then asked whether other dynamic cellular structures can be successfully expanded with U-ExM. We first tested different fixation conditions combined with U-ExM on isolated centrioles to assess structural preservation. We found that centrioles fixed with FA or methanol had good overall structural preservation but a reduced centriole diameter, while fixation with paraformaldehyde (PFA) and glutaraldehyde (GA) did not allow full expansion of centrioles (Supplementary Fig. 12). Then we analyzed the effects of the different fixation conditions followed by incubation in AA–FA solution on human cells. We found that all fixation conditions tested preserved microtubules, and that fixation with both PFA and GA was best suited for structural preservation of mitochondria (Supplementary Fig. 13). Thus, we carried out U-ExM with fixed mammalian cells and analyzed microtubules, mitochondria, and clathrin-coated pits as another membrane-bound structure. We found that U-ExM nicely expanded methanol-fixed microtubules with a full width at half-maximum (FWHM) of 46 nm, in agreement with results from previous ExM methods[4,5,17,18], as well as human centrioles with an average diameter of 190 ± 8 nm (Fig. 3a–d, Supplementary Figs. 14 and 15). Similarly, mitochondria fixed with PFA and GA could be expanded via U-ExM with good structural organization, with the outer mitochondrial membrane translocase TOMM20 surrounding the overall MitoTracker signal (Fig. 3e–h and Supplementary Fig. 16). For both microtubules and mitochondria, U-ExM showed uniform expansion with minimal distortions of 1.6% (microtubules) and 5% (mitochondria), similar to observations from other expansion methods (Supplementary Fig. 17). Finally, we found that FA-fixed clathrin-coated pits could also be visualized as hollow vesicles with U-ExM (Supplementary Fig. 18).

Our results show that ExM protocols have to be carefully optimized to enable isotropic expansion of molecular assemblies. We have demonstrated that U-ExM preserves ultrastructural details and can thus be used successfully to visualize the molecular architecture of diverse multiprotein complexes. In comparison with standard ExM protocols[3,4,17,18], U-ExM alleviates antibody competition

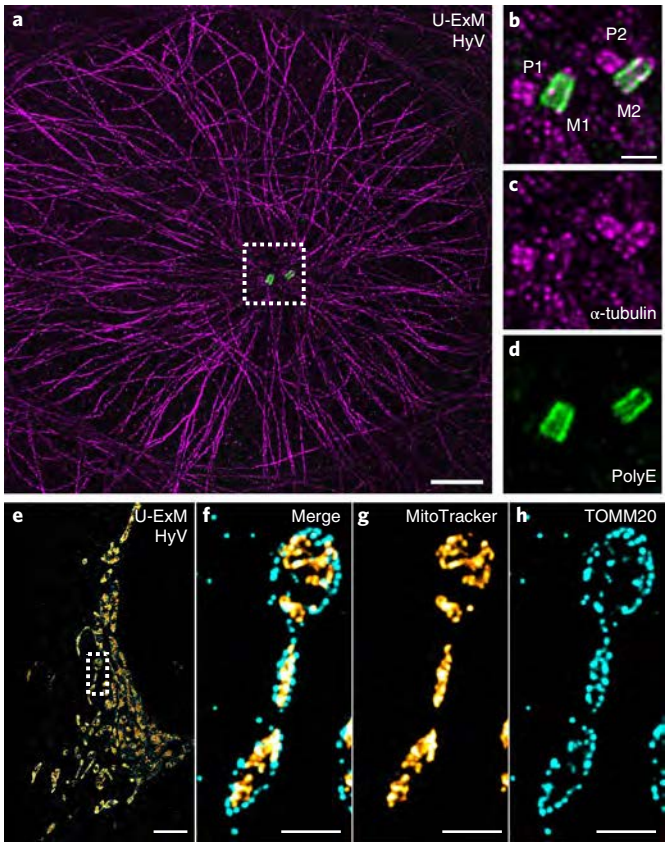

Fig. 3 | U-ExM applied to human cells. a, Representative HyVolution (HyV) confocal image of a U2OS cell fixed with methanol, expanded with U-ExM, and stained for α-tubulin (magenta) and PolyE (green). Scale bar, 10 µm. **b**–**d**, Magnified views of the centriolar pair visible within the dotted square in **a**. P, procentriole; M, mature centriole. Scale bar, 2 µm. Representative images from 3 independent experiments. **e**–**h**, Representative HyVolution confocal images of a U2OS cell fixed with PFA + GA and stained for MitoTracker (orange) and the outer membrane mitochondrial translocase TOMM20 (cyan). Scale bars, 12 µm (**e**) or 3 µm (**f**–**h**). The dotted square in **e** outlines the region shown at higher magnification in **f**–**h**. Note that as expected, the TOMM20 signal surrounds the MitoTracker signal. Representative images from 1 experiment.

and prevents fluorophore loss due to post-expansion labeling. By avoiding chemical fixation of isolated protein complexes, U-ExM improves structural integrity, as demonstrated with isolated centrioles. Notably, in standard ExM approaches, the relative distance of the fluorophore to the epitope stays unchanged, whereas post-expansion labeling approaches led to a relatively smaller antibody size compared with that in the expanded sample. Thus, U-ExM coupled with STED imaging can unveil the chirality of the centriole, a structural feature that previously was revealed by super-resolution microscopy only in appendage proteins radiating 50–100 nm out of the centriole[19]. We are convinced that in the near future U-ExM will be combined with single-molecule localization microscopy to enable fluorescence imaging of molecular details with unsurpassed spatial resolution.

Online content

Any methods, additional references, Nature Research reporting summaries, source data, statements of data availability and associated accession codes are available at https://doi.org/10.1038/s41592-018-0238-1.

Received: 30 April 2018; Accepted: 31 October 2018;
Published online: 17 December 2018

References

1. Koster, A. J. & Klumperman, J. *Nat. Rev. Mol. Cell Biol.* **4**, SS6–SS10 (2003).
2. Sahl, S. J., Hell, S. W. & Jakobs, S. *Nat. Rev. Mol. Cell Biol.* **18**, 685–701 (2017).
3. Chen, F., Tillberg, P. W. & Boyden, E. S. *Science* **347**, 543–548 (2015).
4. Chozinski, T. J. et al. *Nat. Methods* **13**, 485–488 (2016).
5. Tillberg, P. W. et al. *Nat. Biotechnol.* **34**, 987–992 (2016).
6. Ku, T. et al. *Nat. Biotechnol.* **34**, 973–981 (2016).
7. Hamel, V. et al. *Curr. Biol.* **27**, 2486–2498 (2017).
8. Klena, N. et al. *J. Vis. Exp.* **2018**, e58109 (2018).
9. Heilemann, M. et al. *Angew. Chem. Int. Ed. Engl.* **47**, 6172–6176 (2008).
10. Fortun, D. et al. *IEEE Trans. Med. Imaging* **37**, 1235–1246 (2018).
11. Heine, J. et al. *Proc. Natl Acad. Sci. USA* **114**, 9797–9802 (2017).
12. Pigino, G. et al. *J. Cell. Biol.* **195**, 673–687 (2011).
13. Lechtreck, K. F. & Geimer, S. *Cell Motil. Cytoskeleton* **47**, 219–235 (2000).
14. Kubo, T., Yanagisawa, H. A., Yagi, T., Hirono, M. & Kamiya, R. *Curr. Biol.* **20**, 441–445 (2010).
15. Kubo, T. & Oda, T. *Mol. Biol. Cell.* **28**, 2260–2266 (2017).
16. Suryavanshi, S. et al. *Curr. Biol.* **20**, 435–440 (2010).
17. Gao, M. et al. *ACS Nano* **12**, 4178–4185 (2018).
18. Halpern, A. R., Alas, G. C. M., Chozinski, T. J., Paredez, A. R. & Vaughan, J. C. *ACS Nano* **11**, 12677–12686 (2017).
19. Yang, T. T. et al. *Nat. Commun.* **9**, 2023 (2018).

Acknowledgements

We thank N. Klena for critical reading of the manuscript. We thank the BioImaging Center (University of Geneva) for help in image acquisition. We thank the Martinou lab and especially S. Zaganelli for helpful discussions and sharing of mitochondrial reagents. Human U2OS cells were a gift from E. Nigg (Biozentrum, University of Basel, Basel, Switzerland). D.G. and M.S.-C. are supported by the European Research Council (ERC; StG 715289 (ACCENT)). P.G., V.H., and M.L.G. are supported by the Swiss National Science Foundation (SNSF; PP00P3_157517). F.U.Z. and M.S. acknowledge support by the Deutsche Forschungsgemeinschaft (DFG) within the Collaborative Research Center 166 ReceptorLight (projects A04 and B04). M.U. is supported by the ERC (GA No. 692726 GlobalBioIm).

Author contributions

D.G., F.U.Z., M.S., V.H., and P.G. conceived and designed the project. M.S., V.H., and P.G. supervised the project. D.G. and F.U.Z. performed all ExM experiments. D.G. performed all U-ExM experiments with the help of S.B., as well as the data analysis. F.U.Z. performed the dSTORM imaging and the experiment and analysis involving clathrin-coated pits. J.H., J.-G.S., and M.R. performed and analyzed the STED imaging. D.F. and M.U. performed the 3D averaging. M.S.-C. initiated the U-ExM project. M.L.G. performed the plot profile of the polar transform showing the ninefold symmetry, as well as the r.m.s. calculation. E.S.B. helped in setting up ExM. All authors wrote and revised the final manuscript.

Competing interests

The authors declare no competing interests.

Additional information

Supplementary information is available for this paper at https://doi.org/10.1038/s41592-018-0238-1.

Reprints and permissions information is available at www.nature.com/reprints.

Correspondence and requests for materials should be addressed to M.S. or V.H. or P.G.

Publisher's note: Springer Nature remains neutral with regard to jurisdictional claims in published maps and institutional affiliations.

Methods

Reagents. FA (36.5–38%; F8775), sodium acrylate (SA; 97–99%; 408220), guanidine hydrochloride (8 M; G7294), AA (40%; A4058), *N*,*N*′-methylenebisacrylamide (BIS; 2%; M1533), PIPES (P6757), and poly-d-lysine (A-003-E) were purchased from Sigma-Aldrich. Proteinase K (>600 U/mL; EO0491), ammonium persulfate (APS; 17874), tetramethylethylenediamine (TEMED; 17919), DMEM supplemented with GlutaMAX (61965), FBS (10270), and penicillin–streptomycin (15140) were obtained from Thermo Fisher. We used DMEM/HAM's F12 with l -glutamine (Sigma; D8062) supplemented with 10% FBS (Sigma; F7524), penicillin (100 U/ml), and streptomycin (0.1 mg/ml) (Sigma, R8758). PFA (15700) and GA (25%; 16200) were purchased from Electron Microscopy Sciences. Sodium dodecyl sulfate (SDS), Triton X-100, and Tween-20 were obtained from AppliChem, and Tris was obtained from Biosolve. Nuclease-free water (AM9937) was purchased from Ambion–Thermo Fisher. TetraSpeck 0.1-µm fluorescent beads (T7279) were obtained from Thermo Fisher. BSA was purchased from Roche (reference 001,10,086,735). Cytoskeleton buffer comprised the following: 10 mM MES (M8250; Sigma), 150 mM NaCl (Sigma), 5 mM EGTA (67–42–5; Sigma), 5 mM glucose (Sigma; G8270), and 5 mM $MgCl_2$ (ApliChem; A4425), pH 6.1 (NaOH).

SA was diluted with nuclease-free water at a concentration of 38% (wt/wt) and stored at 4 °C for 6 months. Monomer solutions (MSs) of AA and SA were premixed in different ratios and concentrations according to ExM, MAP, and U-ExM protocols and kept as aliquots at –20 °C. MSs were thawed and cooled at 4 °C before gel synthesis. The free-radical initiator APS and polymerization catalyst TEMED were prepared as 10% (wt/wt) stock solutions in nuclease-free water and frozen at –20 °C. For polymerization, APS and TEMED stocks were thawed and chilled on ice before being added to MSs in the desired concentrations. For the ExM protocol, proteinase K was added to freshly prepared digestion buffer directly before use. For the MAP and U-ExM protocols, PFA–AA and FA–AA solutions were prepared freshly before use.

Coverslips used for either sample loading (12 mm) or image acquisition (24 mm) were first washed with absolute ethanol and subsequently dried. Next, coverslips were coated with poly-d-lysine (0.1 mg/ml) and incubated for 1 h either at room temperature (RT) (12-mm coverslips) or at 37 °C (24-mm coverslips), washed three times with ddH_2O, and stored at 4 °C for 1 week.

For immunolabeling, the following primary and secondary antibodies were used in this study: rabbit polyclonal anti-polyglutamate chain (PolyE, IN105) (1:500; AG-25B-0030-C050; Adipogen), mouse monoclonal anti-α-tubulin (DM1α) (1:500; T6199; Sigma-Aldrich), rat monoclonal anti-α-tubulin (YL1/2) (1:500; ab6160; Abcam), rabbit monoclonal anti-TOMM20 (EPR15581-39) (1:200 for non-expanded cells or 1:100 for U-ExM; ab186734; Abcam), mouse anti-α -tubulin (B-5-1-2) (6.7 mg/ml; 1:500; T5168; Sigma), rabbit anti-clathrin heavy chain (1.0 mg/ml; 1:500; Abcam), MitoTracker Red CMXRos (100 nM; M7512; Invitrogen/Thermo Fisher), goat anti-rabbit Alexa Fluor 488 IgG (H + L) (A11008), goat anti-mouse Alexa Fluor 488 IgG (H + L) (A11029), goat anti-mouse Alexa Fluor 568 IgG (H + L) (A11004) (1:400; Invitrogen/Thermo Fisher), and anti-rat Cy3 (1:400; Jackson ImmunoResearch). We also used Alexa Fluor 488 $F(ab')_2$ of goat anti-rabbit IgG (2 mg/ml; 1:200; A11070; Thermo Fisher), Se Tau-647-NHS (K9-4149; SETA BioMedicals) conjugated to $F(ab')_2$ of goat anti-rabbit IgG (SA5-10225; Thermo Fisher) (1.5 mg/ml; 1:200), and DNA dye Hoechst 3342 (10.0 mg/ml; 1:1,000; C10340; Invitrogen). Secondary antibodies anti-rabbit STAR 580 and anti-mouse STAR RED (1:400; Abberior) were used for STED acquisition. Alexa Fluor 647–conjugated $F(ab')_2$ of goat anti-rabbit IgG (2 mg/ml; 1:200; A-21246; Thermo Fisher) was used for dSTORM imaging.

***Chlamydomonas* centriole isolation and centrifugation on coverslips.** *Chlamydomonas* centrioles were isolated from the cell-wall-less *Chlamydomonas* strain $CW15^-$ and spun on coverslips as previously described[8]. Coverslips were then processed either for regular immunofluorescence or for ExM protocols.

Immunofluorescence of non-expanded isolated centrioles. Coverslips with isolated centrioles were fixed with 4% FA in PBS for 10 min at RT and washed in PBS. Coverslips, with centrioles facing down, were then placed on 75 µl of the primary antibody solution diluted in 2% PBS/BSA for 1 h at RT in a humid chamber. Coverslips were then washed in PBS three times for 5 min and subsequently incubated for 1 h at RT with 75 µl of the secondary antibody solution diluted in 2% PBS/BSA in a humid chamber, protected from light. Finally, coverslips were washed in PBS three times for 5 min. Coverslips were then mounted on a glass slide with 6 µl of DABCO containing mounting medium.

Expansion microscopy (ExM) protocol. Centrioles were processed as indicated above for immunofluorescence. After the last PBS wash, coverslips were incubated for 10 min at RT in 0.25% GA in PBS in a six-well plate, washed in PBS three times for 5 min, and then processed for gelation. A small plastic box was covered with Parafilm and put on ice to create a flat hydrophobic surface for gelation. A drop of 35 µl of ExM MS (8.625% (wt/wt) SA, 20% (wt/wt) AA, 0.075% (wt/wt) BIS, 2 M NaCl in 1× PBS) supplemented with 0.2% APS and 0.2% TEMED, with the initiator (APS) added last, was placed on the chilled Parafilm, and coverslips were carefully put on the drop with centrioles facing the gelling solution. Gelation proceeded for 1 min on ice, and then samples were incubated at 37 °C in the dark for 1 h. Then coverslips with attached gels were transferred into a six-well plate for incubation in 2 ml of digestion buffer (1× TAE buffer, 0.5% Triton X-100, 0.8 M guanidine hydrochloride, pH ~8.3) supplemented with fresh proteinase K at 8 units/ml for 45 min at 37 °C. Finally, gels were removed with tweezers from the coverslips and placed in beakers filled with ddH_2O for expansion. Water was exchanged at least twice every 30 min, and then samples were incubated in ddH_2O overnight at RT. Gels expanded between 4× and 4.2× according to SA purity.

MAP protocol. Coverslips with isolated centrioles were incubated in a solution of 4% PFA with 30% AA in PBS for 4–5 h at 37 °C, without a fixation step. Incubation time in PFA–AA was shortened compared with that in the original 'cultured cell' MAP protocol[6] to allow the approach to be adapted to smaller specimens such as isolated centrioles. Immediately after PFA–AA incubation, gelation was carried out as described above for the ExM protocol. Coverslips with centrioles facing down were placed on 35 µl of MAP MS (7% (wt/wt) SA, 20% (wt/wt) AA, 0.1% (wt/wt) BIS in 1× PBS) supplemented with 0.5% APS and 0.5% TEMED, with the initiator (APS) added last, on Parafilm in a precooled humid chamber. Gelation proceeded for 1 min on ice and then shifted to 37 °C in the dark for 1 h. Coverslips with gels were then incubated in ~2 ml of denaturation buffer (200 mM SDS, 200 mM NaCl, and 50 mM Tris in nuclease-free water, pH 9) in a six-well plate for 15 min at RT. Gels were then removed from the coverslips with tweezers, moved into a 1.5-ml Eppendorf centrifuge tube filled with fresh denaturation buffer, and incubated at 95 °C for 30 min. After denaturation, gels were placed in beakers filled with ddH_2O for an initial expansion. Water was exchanged at least twice every 30 min at RT. Successively, gels were placed in PBS two times for 15 min to remove excess water before incubation with primary antibody solution. In this step, gels shrank back to ~50% of their expanded size. Next, gels were incubated with primary antibody diluted in 2% PBS/BSA overnight at RT, with gentle shaking. Gels were then washed in PBS + 0.1% Tween 20 (PBST) three times for 10 min with shaking, and then were incubated with secondary antibody solution diluted in 2% PBS/BSA for ~6 h at RT with gentle shaking. Gels then were washed in PBST three times for 10 min with shaking, and finally were placed in beakers filled with ddH_2O for the final expansion. Water was exchanged at least twice every 30 min, and then gels were incubated in ddH_2O overnight. Gels expanded between 3.3× and 3.5× according to SA purity.

U-ExM protocol. In U-ExM, the sample was not fixed or was mildly fixed prior to expansion. First, coverslips with unfixed isolated centrioles were incubated in a solution of 0.7% FA with 0.15% or 1% AA in PBS for 4–5 h at 37 °C. Next, similar to the ExM and MAP protocols, gelation was carried out via incubation of coverslips with centrioles facing down with 35 µl of U-ExM MS composed of 19% (wt/wt) SA, 10% (wt/wt) AA, 0.1% (wt/wt) BIS in 1× PBS supplemented with 0.5% APS and 0.5% TEMED, on Parafilm in a pre-cooled humid chamber. Note that APS was added last. Importantly, the MS was adapted specifically for U-ExM to achieve an expansion factor of approximately fourfold. Briefly, to find the best expansion conditions, we increased SA and reduced AA concentrations in the MS. We tested the following combinations to compare gel expansion: 20% AA and 7% SA (original MAP MS), 10% AA and 7% SA, 10% AA and 19% SA (U-ExM MS), 5% AA and 7% SA, and 5% AA with 19% SA (Supplementary Fig. 19). Isolated centrioles were then embedded in gels made with MSs with the different AA–SA combinations and expanded to check their quality. The shape of expanded centrioles looked preserved only in gels made with 10% AA (Supplementary Fig. 19). Two independent experiments were performed for each condition.

Gelation proceeded for 1 min on ice, and then samples were incubated at 37 °C in the dark for 1 h. Coverslips with gels were then transferred into ~2 ml of denaturation buffer (200 mM SDS, 200 mM NaCl, and 50 mM Tris in ultrapure water, pH 9) in a six-well plate for 15 min at RT. Gels were then removed from the coverslips with flat tweezers, moved into a 1.5-ml Eppendorf centrifuge tube filled with fresh denaturation buffer, and incubated at 95 °C for 30 min. After denaturation, gels were placed in beakers filled with ddH_2O for the first expansion. Water was exchanged at least twice every 30 min at RT, and then gels were incubated overnight in ddH_2O. Next, to remove excess water before incubation with primary antibody solution, gels were placed in PBS two times for 15 min. Note that in this step, gels shrank back to ~50% of their expanded size. Incubation with primary antibody diluted in 2% PBS/BSA was carried out at 37 °C for ~3 h, with gentle shaking. Gels were then washed in PBST three times for 10 min with shaking and subsequently incubated with secondary antibody solution diluted in 2% PBS/BSA for ~3 h at 37 °C with gentle shaking. Gels were then washed in PBST three times for 10 min with shaking and finally placed in beakers filled with ddH_2O for expansion. Water was exchanged at least twice every 30 min, and then gels were incubated in ddH_2O overnight. Gel expanded between 4.0× and 4.5× according to SA purity.

Mounting and image acquisition. Before imaging, we measured gel size accurately with a caliper to calculate the expansion factor. The gel was then cut with a razor blade into pieces that fit in a 36-mm metallic chamber for imaging. We carefully removed excess water from the piece of gel by placing it between two laboratory wipes. The piece of gel was then mounted on a 24-mm round #1.5 (high-precision)

poly-d-lysine-coated coverslip, already inserted in the metallic chamber, and gently pressed with a brush to ensure adherence of the gel to the coverslip. This step is crucial to completely avoid gel drift during imaging. After a few seconds, a couple of drops of ddH_2O were slowly added on top of the sample until the gel was completely covered with water, to avoid shrinking of the polymer. Confocal microscopy was performed on a Leica TCS SP8 with a 63×/1.4-NA (numerical aperture) oil-immersion objective, using the HyVolution mode[20] to generate deconvolved images, with the following parameters: 'HyVolution Grade' at max resolution, Huygens Essential as 'Approach', water as 'Mounting Medium', and Best Resolution as 'Strategy'. 3D *z*-stacks at 0.12-µm intervals were acquired with a pixel size of 35 nm.

For post-U-ExM imaging of clathrin, microutubles, and DNA, we used a rescanning confocal microscope (RCM), which is based on the image-scanning principle whereby pixel reassignment is achieved purely optomechanically[21]. The RCM unit (Confocal.nl) is attached to a side port of a Nikon TiE and equipped with an sCMOS (scientific complementary metal-oxide semiconductor) Zyla 4.2 P (Andor). The pinhole is fixed at a 50-µm pinhole size. As an excitation source, the laser unit Cobolt Skyra (Cobolt, Hübner Group) is fiber-coupled and connected to the RCM unit. The laser unit has four laser lines (405 nm, 488 nm, 561 nm, and 640 nm) with 50 mW each (free beam). Various OD filters are introduced in the excitation path to attenuate the laser power. The TiE is equipped with a motorized stage (Nikon) and a 60× water-immersion objective (CFI Plan APO, 1.27-NA; Nikon). The setup is fully controlled with NIS-Elements version 4.6 on Windows 8.

STED imaging was performed on a commercial STED microscope (Expert Line, Abberior-Instruments, Germany) working at a repetition rate of 40 MHz (ref. [22]). Centrioles were immunostained with secondary antibodies conjugated to STAR RED and/or Star 580 dye (Abberior, Germany). STAR RED was imaged with excitation at a wavelength of 640 nm and time-gated fluorescence detection between 650 and 720 nm. STAR 580 was excited at 561 nm with time-gated detection between 580 and 630 nm. The STED laser had a wavelength of 775 nm and a pulse width of roughly 500 ps. The pinhole was set to 0.75 Airy units (AU). For imaging, a water-immersion objective lens was used (UPLSAPO 60XW, Olympus, Japan). To arrive at high fluorescence signals and STED resolutions for a clear structure representation, we used the recently published adaptive-illumination scan technique DyMIN[11]. Non-expanded centrioles were imaged with a 100×/1.4-NA oil-immersion objective.

dSTORM imaging was conducted on an inverted microscope (Zeiss Axio Observer.Z1, Carl Zeiss Microscopy) equipped with a 100× oil-immersion objective (alpha Plan-Apochromat 100×/1.46 Oil DIC, Carl Zeiss Microscopy) and a 63× water-immersion objective lens (LD C-Apochromat 63×/1.15 W Corr M27, Carl Zeiss Microscopy). For illumination of the sample, a 640-nm diode laser (iBeam smart, Toptica Photonics) was used. The laser beam was adjusted to quasi-TIRF mode for use with the oil-immersion objective and to epifluorescence configuration with the water-immersion objective. Between 20,000 and 40,000 frames were collected on an EM-CCD (electron-multiplying charge-coupled device) camera (Andor Ixon Ultra DU897U-CSO) at a frame rate of 50–80 Hz. An autofocus system (Zeiss Definite Focus) kept the focus stable during image acquisition. For 3D imaging, a cylindrical lens ($f = 250$ mm) was placed in the detection path of the microscope setup. Samples were placed in freshly prepared photoswitching buffer consisting of 100 mM cysteamine hydrochloride (Sigma) in PBS (1×), pH 7.5, supplemented with an oxygen scavenger system (2% glucose (w/v), 2 U/ml glucose oxidase (Sigma), and 200 U/ml catalase (Sigma)). 2D super-resolution images were reconstructed with the ImageJ plugin ThunderSTORM[23], and for 3D images the open-source software rapidSTORM 3.3 (ref. [24]) was used.

Measurements of centriole diameter. We selected only nearly perfect top-view centrioles for measurement of centriole diameter (Supplementary Fig. 2). Briefly, we included in the analysis only centrioles for which the most distal and most proximal regions were aligned. We used the line scan and plot profile tools of Fiji to determine the diameter. For each centriole, a line was drawn through the ninefold-symmetrical PolyE signal clearly seen at the end of the central core, and the distance between the two peaks of intensity was measured. The diameter was obtained from the average of two measurements. Related to Fig. 1, for each condition, three independent experiments were analyzed. PolyE: $n = 30$ centrioles for ExM, MAP, and U-ExM; $n = 15$ for non-expanded dSTORM. Tubulin: $n = 29$ for ExM and U-ExM; $n = 20$ for MAP. Related to Supplementary Fig. 12, FA, $n = 11$ centrioles, 1 experiment; methanol, $n = 16$, 2 independent experiments; PFA/GA, $n = 13$, 1 experiment. Related to Supplementary Fig. 14, the diameter of human centrioles in methanol-fixed U2OS cells was calculated from 13 centrioles from 1 experiment.

Isotropic expansion of centrioles. We determined the isotropic expansion by comparing the length-to-diameter ratio of expanded centrioles to that of non-expanded centrioles. We used the line scan and plot profile tools of Fiji to measure the length and diameter of α-tubulin staining in nearly perfect lateral views of centrioles. For length determination, a line scan of a size able to cover the whole width of the centriole was drawn in a maximum projection image, and the distance between the first peak and the last peak of intensity was measured. Measurements of the diameter were performed as described above. For each condition, three independent experiments were analyzed, except for the structured illumination microscopy experiment, which was performed once. $N = 30$ centrioles for ExM and MAP, $n = 29$ for U-ExM, and $n = 22$ for non-expanded structured illumination microscopy.

Analysis of the centriolar ninefold symmetry. To graphically quantify the ninefold symmetry of the PolyE signal, we used the Polar Transformer plugin (https://imagej.nih.gov/ij/plugins/polar-transformer.html) and the line scan and plot profile tools of Fiji. For each centriole, a single *z* plane (the same *z* plane used to quantify the centriole diameter) was transformed to polar coordinates with the Polar Transformer plugin, generating 'unwrapped' images (Supplementary Fig. 3c). Then a straight line wide enough to cover the whole signal was drawn to obtain the plot profile. Curves from 30 centrioles for each condition from three independent experiments were merged to create a unique averaged curve as follows. A sinusoidal model was generated to represent a theoretical plot profile of a polar-transformed centriole. This model is described by the following formula:

$$f(x) = 0.5 + 0.5\sin\left(\frac{2\pi}{\text{Period}}x\right)$$

where the period can be calculated by dividing the length of an experimental plot profile by 9. To compare an experimental centriole plot profile to this model, we rescaled the experimental values between 0 and 1. Then, the plot profile was progressively moved along its *x* axis. For each shift, the cross-correlation between the experimental data and the model was calculated. The shift value giving the best cross-correlation was conserved, and the plot profile was moved according to it. Once all plot profiles had been aligned on the sinusoidal model, an average profile was generated. The model and the cross-correlation search were done using the language R.

Analysis of centriolar shape. We used the shape descriptor tool of Fiji to analyze centriole shape quality. The single *z* plane already used to measure centriole diameter was also used to analyze centriole shape. Using PolyE staining, we drew a polygon with nine vertexes around the circumference, joining the nine microtubule triplets when visible. The shape descriptor tool gives several parameters, among them the roundness value, defined as the ratio of minor axis to major axis for the figure. A value of 1 represents a perfectly round shape. For each condition, we analyzed 30 centrioles from three independent experiments.

Comparison between dSTORM and U-ExM. Isolated centrioles, either non-expanded or expanded via the U-ExM protocol, were stained for PolyE and imaged with dSTORM or confocal microscopy, respectively. A straight line that bisected the microtubule triplets of procentrioles was drawn with the line tool in Fiji. Then we used the line scan and plot profile tools to measure the fluorescence profile along this line and obtain the FWHM of the curve for dSTORM (4 non-expanded procentrioles, total of 24 triplets, one experiment), U-ExM + confocal microscopy (9 expanded procentrioles, total of 76 triplets, 3 independent experiments), and U-ExM + HyVolution (9 expanded procentrioles, total of 81 triplets, 3 independent experiments). Analysis was performed on the maximum-intensity projection of 3D stack acquisitions. To monitor the ninefold symmetry of the PolyE signal, we used the Polar Transformer plugin in Fiji as described above.

Isotropic 3D averaging. We obtained particle averaging results for isolated *C. reinhardtii* centrioles by using the method described in ref. [10]. We used the StackReg plugin[25] for data preprocessing to correct drifts between slices of the image stacks. We averaged 14 centrioles from one experiment that we selected with the software ImageJ. To model the point spread function (PSF), we acquired images of 0.1-µm fluorescent beads embedded in a U-ExM gel. We obtained the final PSF volume by registering and averaging 15 images of beads.

The reconstruction was realized in two steps. The first step used as input the PSF model and a restricted number L of particles representing the main orientations to create a coarse initial reconstruction without reference. Because of the cyclical symmetry of the centriole, most of the information can be captured from top and side views, which corresponds to $L = 2$. We downsampled the input volumes by a factor of 2 to accelerate computations. We used the bi-level and block-coordinate optimization approach described in ref. [10]. To further speed up the computations, we replaced the stochastic optimization approach for the estimation of pose parameters by a deterministic search with coarse discretization. The second step refined the result of the first step by considering all the available data and a more accurate model. The volume and particle poses were alternately updated until convergence. In both steps, we applied a C9 symmetry constraint to the reconstructed volumes. The custom Matlab source code is available at https://github.com/dfortun2/U-ExM. The reconstruction code with known angles uses the inverse problem library GlobalBioIm[26]. The parameters used for the reconstruction of Supplementary Fig. 6 are the default parameters accessible in the code.

Sub-triplet localization analysis. Isolated centrioles were expanded via the U-ExM protocol, costained for PolyE and α-tubulin, and imaged with a confocal microscope. Before analysis, deconvolution was applied on images. A straight line that bisected the microtubule triplets from the inside toward the outside was drawn with the line tool in Fiji[27]. Then, the line scan and plot profile tools were used to measure the fluorescence profiles of PolyE and α-tubulin along the same line and normalize them on the highest value (Supplementary Fig. 7a–d). Both curves were aligned on the peak of PolyE as a reference point. $N=8$ centrioles from 3 independent experiments, for a total of 61 microtubule triplets.

To model the position of the fluorescence signal in the centriole, we scaled a 2D image extracted from cryo-EM data to obtain a centriole with the expanded diameter after expansion. The resulting image gave a centriole with a diameter of 1,125 nm (Supplementary Fig. 7e) (centriole diameter × expansion factor = 250 nm × 4.5 = 1,125 nm). We repeated the same operation for A-, B-, and C-microtubules (Supplementary Fig. 7f–h). These images were then filtered at the resolution of HyVolution (140 nm) with a bandpass filter in ImageJ (Supplementary Fig. 7i–l). We generated the final images (Supplementary Fig. 7m–o) by merging each specific microtubule signal (Supplementary Fig. 7j–l) on the initial microtubule triplet image (Supplementary Fig. 7i). Sub-triplet localization analysis was done as described above.

Cryo-electron microscopy of *Chlamydomonas* centrioles. Isolated *Chlamydomonas* centrioles[8] were applied to lacey carbon film grids (300Mesh, EMS), vitrified in liquid ethane. Grids were transferred to a JEM 2200FS cryo-electron microscope (JEOL) operating at 200 keV and equipped with a field emission gun. Images were collected with a 2,048 × 2,048 CCD camera (Gatan).

Quantification of microtubule-triplet angle. We used the angle tool in Fiji[27] to measure the angle between the center of the centriole and the microtubule triplets. $N=77$ microtubule triplets for electron microscopy images and $n=65$ for U-ExM. Data from one experiment.

Chlamydomonas culture and expansion. *Chlamydomonas* cells were cultured in Tris acetate phosphate medium for 3 d at 23 °C (ref. [8]). Cells were allowed to adhere to 12-mm poly-d-lysine-coated coverslips for 15 min. We used this procedure, instead of spinning cells onto the coverslip, to increase the chance of finding flagella positioned perpendicularly to the focal plane and to prevent deflagellation due to the centrifugation. Coverslips were next processed via the U-ExM protocol. 3D rendering was done with the ImageJ[28] plugin ClearVolume[29].

Measurements of flagellum diameter. *Chlamydomonas* cells expanded via the U-ExM protocol were costained for PolyE and α-tubulin and imaged with a confocal microscope. Before analysis, deconvolution was applied to images. We selected only nearly perfect cilia cross-sections for measurement of the diameter. The diameter was quantified with the use of the line scan and plot profile tools of Fiji[27]. For each cilium, a line that bisected the center of the cilium was drawn, and the fluorescence profiles of both PolyE and α-tubulin were measured along this line. A curve for each cilium was obtained from the average of two measurements and normalized on the highest value, for both stainings. All curves were then aligned, with the center between the two peaks of intensity used as a reference point. $N=23$ flagella from 3 independent experiments were analyzed.

The modeling of PolyE on the B-microtubule (half or full) was done similarly to the sub-triplet localization on centrioles. Briefly, a cryo-EM image of a cilium cross-section was scaled to obtain a cilium with a diameter of 900 nm (cilium diameter × expansion factor = 200 nm × 4.5 = 900 nm). These images were then filtered at the resolution of HyVolution (140 nm) with a bandpass filter in ImageJ.

Quantification of PolyE signal in *Chlamydomonas* flagella. Polyglutamylation of doublets and central-pair microtubules of *Chlamydomonas* flagella was analyzed on sprayed flagella (Supplementary Fig. 11a–f). For each flagellum, using the software Fiji[27], we drew a line scan of a few micrometers across the nine microtubule doublets (MTDs) and two central-pair microtubules to measure the plot profile of the PolyE signal. Next, we obtained the average of the nine intensity peaks of the MTDs and the average of the two intensity peaks of the central-pair microtubules. Finally, we calculated the ratio between the PolyE signal at the MTDs and that at the central-pair microtubules for each flagellum and obtained the average for four sprayed flagella from one experiment.

Immunofluorescence of human cells. Human U2OS cells (a gift from Erich Nigg) were seeded at a density of ~100,000 cells per well in a six-well plate containing 12-mm coverslips and incubated overnight at 37 °C with 5% CO_2 in DMEM supplemented with GlutaMAX, 10% FBS, and penicillin–streptomycin (100 µg/ml). To investigate the effect of fixation on microtubule preservation, we tested four different conditions: cells were (1) transferred into a solution of 0.7% FA and 1% AA in PBS (AA–FA U-ExM solution) without fixation, (2) fixed for 7 min in −20 °C methanol, (3) fixed with 4% FA in CS buffer (10 mM MES, 150 mM NaCl, 5 mM EGTA, 5 mM glucose, 5 mM $MgCl_2$, pH 6.1) for 10 min at RT, or (4) rapidly pre-extracted in BRB80 solution with 0.5% Triton and fixed with 3% PFA + 0.1% GA in PBS for 15 min at RT. After fixation, cells were quickly washed in PBS and then incubated for 5 h in AA–FA U-ExM solution at 37 °C. Next, coverslips were incubated with primary antibody diluted in antibody solution (PBS with 1% BSA and 0.05% Tween) for 1 h at RT in a humid chamber. For condition (1), cells were rapidly pre-extracted in BRB80 solution with 0.5% Triton before incubation with the primary antibody solution. Coverslips were then washed in PBS three times for 5 min and subsequently incubated for 1 h at RT with secondary antibody diluted in antibody solution in a humid and dark chamber. Finally, coverslips were washed in PBS three times for 5 min, quickly dried, and mounted on a glass slide with 3 µl of DABCO containing mounting medium.

Similarly, we tested the effects of fixation on the preservation of mitochondria under four different conditions. Cells were first incubated for 15 min with MitoTracker (100 nM, diluted in the culturing medium) and then were (1) transferred into AA–FA U-ExM solution without fixation, (2) fixed for 7 min in −20 °C methanol, (3) fixed with 4% FA in PBS for 15 min at RT, or (4) fixed with 3% PFA + 0.1% GA in PBS for 15 min at RT. After fixation, cells were briefly washed in PBS and then were incubated with permeabilization/blocking buffer (PBS with 3% BSA; 0.3% Triton) for 30 min. Next, cells were rapidly washed in PBS and then transferred into AA–FA U-ExM solution for 5 h at 37 °C. Finally, coverslips were briefly washed in PBS, quickly dried, and mounted on a glass slide with 3 µl of DABCO containing mounting medium.

Pre- and post-U-ExM assessment of microtubules and mitochondria in human cells. Human U2OS cells were grown as described above. In this case, cells were seeded in a six-well plate containing 24-mm round #1.5 (high-precision) coverslips. To compare microtubules pre- and post-U-ExM, we fixed cells in −20 °C methanol for 7 min and then incubated them in AA–FA U-ExM solution for 5 h at 37 °C. Next, cells were stained with rat anti-α-tubulin (YL1/2) and secondary Cy3 as described above and imaged. Next, coverslips were processed via the U-ExM protocol, with the following differences: gelation was allowed to initiate on ice for 5 min before incubation at 37 °C, 140 µl of U-ExM MS supplemented with 0.5% APS and 0.5% TEMED was used, and denaturation proceeded for 1.5 h (a longer time was chosen for cells than for isolated centrioles to ensure maximal expansion in this complex specimen). For post-expansion staining, we used mouse anti-α-tubulin (DM1α) and Alexa Fluor 488.

To compare mitochondria pre- and post-U-ExM, we incubated cells for 15 min with MitoTracker Red CMXRos (100 nM, diluted in the culturing medium), fixed them in 3% PFA + 0.1% GA in PBS for 15 min at RT, and then incubated them in AA–FA U-ExM solution for 5 h at 37 °C. Next, we acquired pre-expansion images. Then the U-ExM protocol was applied similarly as for microtubules, but with denaturation allowed to proceed for 1 h at 70 °C (1.5 h of denaturation completely destroyed mitochondria (data not shown)). For post-expansion staining, rabbit anti-TOMM20 and Alexa Fluor 488 were used. Note that the MitoTracker signal was retained after expansion, and thus was acquired and used to calculate the r.m.s. error between pre- and post-expansion images.

To recognize the region of the coverslip where cells were acquired, we applied a mark to the opposite side of the coverslip where cells were present. This allowed us to cut the piece of gel including only the cells acquired pre-expansion and facilitated their acquisition post-expansion.

Post-U-ExM analysis of clathrin, microtubles, and DNA. For post-U-ExM labeling of clathrin-coated pits, microtubules, and DNA, we cultured COS-7 African green monkey kidney cells (purchased from CLS Cell Line Service GmbH) in DMEM/HAM's F12 with l -glutamine supplemented with 10% FBS, penicillin (100 U/ml), and streptomycin (0.1 mg/ml) at 37 °C and 5% CO_2. We seeded 30,000 cells per well on round 18-mm high-precision coverslips (#1.5) in 12-well culture plates (TPP, 92012). Cells were grown for 24 h at 37 °C and 5% CO_2 and subsequently fixed in 4% FA in cytoskeleton buffer at 37 °C for 10 min. After fixation, cells were briefly washed with PBS and then transferred into AA–FA U-ExM solution for 5 h at 37 °C. Gelation and denaturation of the sample were carried out as described above for pre- and post-U-ExM on human cells, but with 60 µl of U-ExM MS. For post-expansion staining, mouse anti-α-tubulin (B-5-1-2) and anti-clathrin heavy chain were diluted in PBS (1×) and incubated for 3 h at 37 °C simultaneously. Samples were washed in PBST three times for 20 min each time. Then secondary antibodies Al488-F(ab′)$_2$ of goat anti-rabbit IgG and Se Tau-647 conjugated to F(ab′)$_2$ of goat anti-mouse IgG were incubated simultaneously at 37 °C for 3 h in PBS (1×). The gels were washed two times in PBST for 20 min and once in PBS (1×) for 20 min. DNA Hoechst dye in PBS (1×) was incubated for 20 min at room temperature. The gels were then fully expanded in ddH_2O and immobilized on poly-d-lysine-coated 24-mm coverslips as described above. The samples were imaged on an RCM.

Intensity profiles of manually chosen CCPs that showed typical central nulls were analyzed with Fiji. The intensities were normalized to the maximum intensity value, and double Gaussian fits were fitted to the intensity profiles with the software Origin (OriginLab, Northampton, MA). To determine the diameters of the pits, we calculated the distance to the centers of the single Gaussian fits.

The s.e. of the diameter was calculated from the square root of the sum of the squared errors from the center values of the single Gaussian fits.

Distortion analysis. To estimate the sample deformation after expansion, we calculated the r.m.s. error between two images of the same structure before and after expansion, following the protocol described by Chozinski et al[4]. This protocol also provides the scale factor between the images, thus giving the expansion factor of the experiment. For both microtubules and mitochondria, the data from three independent experiments were used.

Statistics and reproducibility. All experiments were carried out three times independently, unless indicated otherwise in the figure legends. All data are expressed as the average (mean) ± s.d. The *n* values, which represent the number of centrioles or the number of triplets analyzed, are stated in figure legends and in the Methods. Statistical one-way ANOVA and unpaired two-tailed *t*-tests were used as indicated in the figure legends.

Reporting summary. Further information on research design is available in the Nature Research Reporting Summary linked to this article.

Code availability. The custom Matlab source code is available at https://github.com/dfortun2/U-ExM.

Data availability

The data that support the findings of this study are available from the corresponding authors upon request.

References

20. Borlinghaus, R. T. & Kappel, C. *Nat. Methods* **13**, i–iii (2016).
21. De Luca, G. M. R. et al. *J. Microsc.* **266**, 166–177 (2017).
22. Göttfert, F. et al. *Proc. Natl Acad. Sci. USA* **114**, 2125–2130 (2017).
23. Ovesný, M., Křížek, P., Borkovec, J., Švindrych, Z. & Hagen, G. M. *Bioinformatics* **30**, 2389–2390 (2014).
24. Wolter, S. et al. *Nat. Methods* **9**, 1040–1041 (2012).
25. Thévenaz, P., Ruttimann, U. E. & Unser, M. *IEEE Trans. Image Process.* **7**, 27–41 (1998).
26. Unser, M., Soubies, E., Soulez, F., McCann, M. & Donati, L. GlobalBioIm: a unifying computational framework for solving inverse problems. *OSA Technical Digest* https://doi.org/10.1364/COSI.2017.CTu1B.1 (2017).
27. Schindelin, J. et al. *Nat. Methods* **9**, 676–682 (2012).
28. Schneider, C. A., Rasband, W. S. & Eliceiri, K. W. *Nat. Methods* **9**, 671–675 (2012).
29. Royer, L. A. et al. *Nat. Methods* **12**, 480–481 (2015).

nature research

Corresponding author(s): Paul Guichard, Virginie Hamel and Markus Sauer

Reporting Summary

Nature Research wishes to improve the reproducibility of the work that we publish. This form provides structure for consistency and transparency in reporting. For further information on Nature Research policies, see Authors & Referees and the Editorial Policy Checklist.

Statistical parameters

When statistical analyses are reported, confirm that the following items are present in the relevant location (e.g. figure legend, table legend, main text, or Methods section).

n/a	Confirmed	
☐	☒	The exact sample size (*n*) for each experimental group/condition, given as a discrete number and unit of measurement
☐	☒	An indication of whether measurements were taken from distinct samples or whether the same sample was measured repeatedly
☐	☒	The statistical test(s) used AND whether they are one- or two-sided *Only common tests should be described solely by name; describe more complex techniques in the Methods section.*
☒	☐	A description of all covariates tested
☒	☐	A description of any assumptions or corrections, such as tests of normality and adjustment for multiple comparisons
☐	☒	A full description of the statistics including central tendency (e.g. means) or other basic estimates (e.g. regression coefficient) AND variation (e.g. standard deviation) or associated estimates of uncertainty (e.g. confidence intervals)
☒	☐	For null hypothesis testing, the test statistic (e.g. *F*, *t*, *r*) with confidence intervals, effect sizes, degrees of freedom and *P* value noted *Give P values as exact values whenever suitable.*
☒	☐	For Bayesian analysis, information on the choice of priors and Markov chain Monte Carlo settings
☒	☐	For hierarchical and complex designs, identification of the appropriate level for tests and full reporting of outcomes
☒	☐	Estimates of effect sizes (e.g. Cohen's *d*, Pearson's *r*), indicating how they were calculated
☐	☒	Clearly defined error bars *State explicitly what error bars represent (e.g. SD, SE, CI)*

Our web collection on statistics for biologists may be useful.

Software and code

Policy information about availability of computer code

Data collection	Centrioles were imaged using a Leica TCS SP8 using a 63x 1.4 NA oil objective, with the HyVolution mode2 to generate deconvolved images, with the following parameters. 'HyVolution Grade' at max Resolution, Huygens Essential as 'Approach', water as 'Mounting Medium' and Best Resolution as 'Strategy'. STED imaging was performed on a commercial STED microscope (Expert Line, Abberior-Instruments, Germany) working at repetition rate of 40 Mhz. dSTORM imaging was conducted on an inverted microscope (Zeiss Axio Observer.Z1, Carl Zeiss Microscopy) equipped with a 100x oil-immersion objective (alpha Plan-Apochromat 100x/1.46 Oil DIC, Carl Zeiss Microscopy) and a 63x water objective lens (LD C-Apochromat 63x/1.15 W Corr M27, Carl Zeiss Microscopy).

Data analysis	The extraction of individual particles in input volumes was realized manually with the software ImageJ, version 1.51s. A drift correction was applied in the acquired stacks of images with the ImageJ plugin StackReg: http://bigwww.epfl.ch/thevenaz/stackreg/. The code for particle averaging was developed by the authors and is available on the GitHub repository: https://github.com/dfortun2/U-ExM. This is a Matlab code, with a graphical interface for each step of the reconstruction. We refer to the README file of the repository for more details. 2D Super-resolution images were reconstructed using the ImageJ plugin ThunderSTORM 5 and for 3D images the open source software rapidSTORM 3.36 was used . The Intensities of clathrin-coated pits were normalized to the maximum intensity value and double guassian fits were fitted to the Intensity profiles using the software Origin (OriginLab, Northampton, MA).

For manuscripts utilizing custom algorithms or software that are central to the research but not yet described in published literature, software must be made available to editors/reviewers upon request. We strongly encourage code deposition in a community repository (e.g. GitHub). See the Nature Research guidelines for submitting code & software for further information.

Data

Policy information about availability of data

All manuscripts must include a data availability statement. This statement should provide the following information, where applicable:

- Accession codes, unique identifiers, or web links for publicly available datasets
- A list of figures that have associated raw data
- A description of any restrictions on data availability

The data that support the findings of this study are available from the corresponding authors upon request.

Field-specific reporting

Please select the best fit for your research. If you are not sure, read the appropriate sections before making your selection.

☒ Life sciences ☐ Behavioural & social sciences ☐ Ecological, evolutionary & environmental sciences

For a reference copy of the document with all sections, see nature.com/authors/policies/ReportingSummary-flat.pdf

Life sciences study design

All studies must disclose on these points even when the disclosure is negative.

Sample size	We analyzed in most experiments around 30 isolated centrioles (10 centrioles per each three independent experiments). Note that we stated in the manuscript how many centrioles were analyzed in each experiment. We did not use a predetermined sample size. Considering the time of acquisition, we acquired 10 centrioles per experiment.
Data exclusions	To measure centriole diameter, we solely quantify nearly perfect top view centrioles to avoid any biais due to tilted centrioles. We stated this in the online methods section (Measurements of centriole diameter) and made a supplementary figure to explain this choice (Supplementary Fig.2). For the in cellulo flagella analysis, we analyzed only fully expanded flagella and we specified this in the online methods section.
Replication	All experiments, imaging and analysis were carried out 3 times independently, unless specified otherwise for Figures 2b, 3b-f, 4c, which were performed once. This is reported in the Online method (statistics and reproducibility).
Randomization	This is not relevant for our study because we selected only nearly perfect top and lateral views of centrioles. In a given gel, centrioles are found in many orientations.
Blinding	Blinding is not relevant for our study for the same reasons as specified above.

Reporting for specific materials, systems and methods

Materials & experimental systems

n/a	Involved in the study
☒	☐ Unique biological materials
☐	☒ Antibodies
☐	☒ Eukaryotic cell lines
☒	☐ Palaeontology
☐	☒ Animals and other organisms
☒	☐ Human research participants

Methods

n/a	Involved in the study
☒	☐ ChIP-seq
☒	☐ Flow cytometry
☒	☐ MRI-based neuroimaging

Antibodies

Antibodies used

-rabbit polyclonal anti-polyglutamate chain (PolyE, IN105), reference AG-25B-0030-C050, Adipogen, dilution 1/500
-mouse monoclonal anti-alpha tubulin (DM1alpha), reference T6199, Sigma, dilution 1/500
-rat monoclonal anti-alpha tubulin (YL1/2), Abcam, ab6160, dilution 1/500
-goat anti-rabbit Alexa Fluor 488 IgG (H+L), Invitrogen A11008, dilution 1/400
-goat anti-mouse Alexa Fluor 488 IgG (H+L), Invitrogen A11029, dilution 1/400
-goat anti-mouse Alexa Fluor 568 IgG (H+L), Invitrogen A11004, dilution 1/400
-anti-rabbit STAR 580, Aberrior, S-12-2015Hp, dilution 1/400
-anti-mouse STAR RED, Aberrior, S-08-2016Hp, dilution 1/400
-A1647 conjugated F(ab')2 fragment of goat anti-rabbit, reference A-21246, ThermoFisher, dilution 1/200
-MitoTracker red CMXRos, M7512, InVitrogen, 100nM
-rabbit monoclonal anti-TOMM20 (EPR15581-39), ab186734 Abcam, dilution 1/200
-anti-rat Cy3, Jackson ImmunoResearch, 712-166-153, dilution 1/400
-mouse anti-alpha tubulin (B-5-1-2) Sigma T5168, dilution 1/500 (6.7mg/ml)
-rabbit anti-clathrin heavy chain, Abcam, dilution 1/500
-Alexa Fluor 488 F(ab`)2 of goat anti rabbit IgG (2mg/ml, 1:200, A11070, ThermoFisher)
-Se Tau-647-NHS (K9-4149, SETA BioMedicals) conjugated to F(ab') 2 of goat anti-Rabbit IgG (SA5-10225, ThermoFisher), 1.5mg/ml, 1/200
-DNA-dye Hoechst 3342, C10340, Invitrogen, 10mg/ml, 1/1000
-Alexa Fluor 647 F(ab`)2 of goat anti rabbit IgG, A-21246, ThermoFisher, 2mg/ml, 1/200

Validation

-PolyE antibody (IN105) recognizes specifically glutamate chains of four or more glutamates. https://adipogen.com/ag-25b-0030-anti-polyglutamate-chain-polye-pab-in105.html/
-DM1A antibody recognizes the following epitope in alpha tubulin: aa 426-450. https://www.sigmaaldrich.com/catalog/product/sigma/t6199?lang=fr&region=CH

Eukaryotic cell lines

Policy information about cell lines

Cell line source(s)

U2OS: cell line provided by Erich Nigg (Biozentrum, Basel, Switzerland). COS-7 were purchased from CLS Cell Line Service GmbH.

Authentication

None of the cell lines used were authenticated

Mycoplasma contamination

U20S cell lines were negative for mycoplasma contamination. COS-7 were not tested for mycoplasma.

Commonly misidentified lines
(See ICLAC register)

Name any commonly misidentified cell lines used in the study and provide a rationale for their use.

Animals and other organisms

Policy information about studies involving animals; ARRIVE guidelines recommended for reporting animal research

Laboratory animals

The cell wall-less Chlamydomonas strain CW15- used in this study was grown in liquid TAP (Tris-acetate-phosphate) buffer at ~22°C or on solid TAP plates with 1.5% agar.

Wild animals

no wild animals were used in this study.

Field-collected samples

no field-collected samples were used in this study.

nature methods

SUPPLEMENTARY INFORMATION

https://doi.org/10.1038/s41592-018-0238-1

In the format provided by the authors and unedited.

Imaging cellular ultrastructures using expansion microscopy (U-ExM)

Davide Gambarotto[1,9], Fabian U. Zwettler[2,9], Maeva Le Guennec[1], Marketa Schmidt-Cernohorska[1,7], Denis Fortun[3,8], Susanne Borgers[1], Jörn Heine[4], Jan-Gero Schloetel[4], Matthias Reuss[4], Michael Unser[5], Edward S. Boyden[6], Markus Sauer[2]*, Virginie Hamel[1]* and Paul Guichard[1]*

[1]Department of Cell Biology, Sciences III, University of Geneva, Geneva, Switzerland. [2]Department of Biotechnology and Biophysics, Biocenter, University of Würzburg, Würzburg, Germany. [3]Signal Processing Core of Center for Biomedical Imaging (CIBM-SP), EPFL, Lausanne, Switzerland. [4]Abberior Instruments GmbH, Göttingen, Germany. [5]Ecole Polytechnique Fédérale de Lausanne (EPFL), Biomedical Imaging Group, Lausanne, Switzerland. [6]Massachusetts Institute of Technology (MIT), Cambridge, MA, USA. [7]Present address: Laboratory of Adaptative Immunity, Institute of Molecular Genetics, Academy of Sciences of the Czech Republic, Prague, Czech Republic. [8]Present address: ICube, CNRS, University of Strasbourg, Illkirch, France. [9]These authors contributed equally: Davide Gambarotto, Fabian U. Zwettler. *e-mail: m.sauer@uni-wuerzburg.de; virginie.hamel@unige.ch; paul.guichard@unige.ch

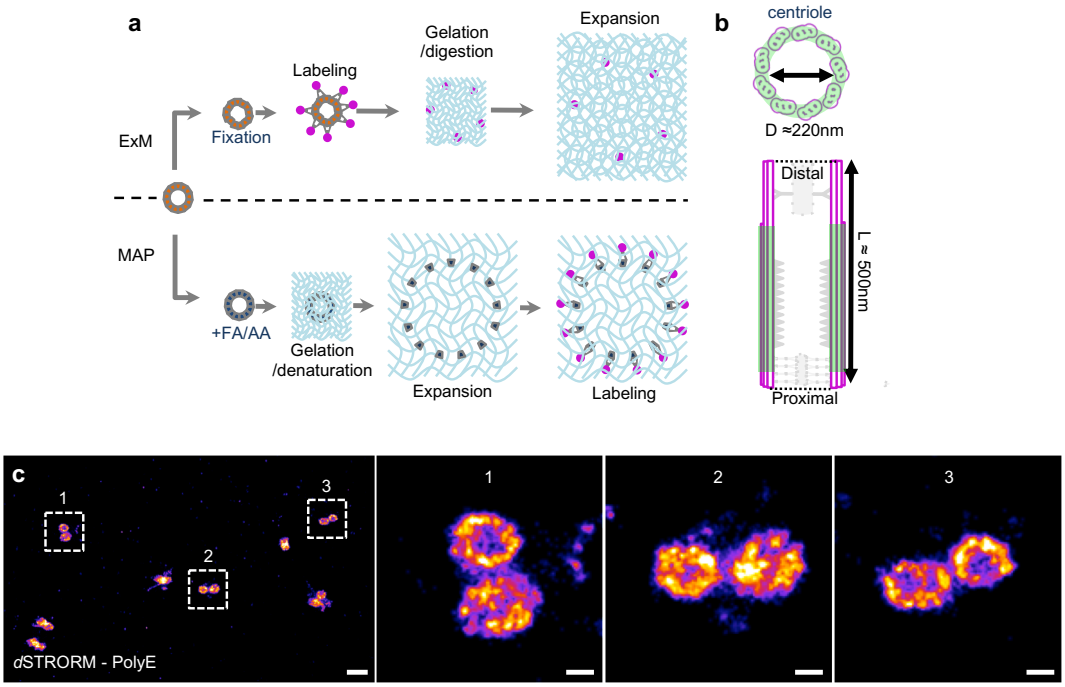

Supplementary Figure 1. Expansion methods and non-expanded centrioles in *d*STORM. (**a**) Schematic illustration of two methods of expansion microscopy, ExM and MAP. (**b**) Schematic representation of a centriole seen either in top view (top) or lateral view (bottom). (**c**) 2D *d*STORM image of isolated *Chlamydomonas* centrioles stained with PolyE (Alexa 647). Scale bar: 400 nm. (1-3) Magnified views of boxed regions of (**c**) Scale bar: 100 nm. Examples of centrioles used to quantify the diameter of non-expanded centriole in **Fig.1**. Representative images from 1experiment.

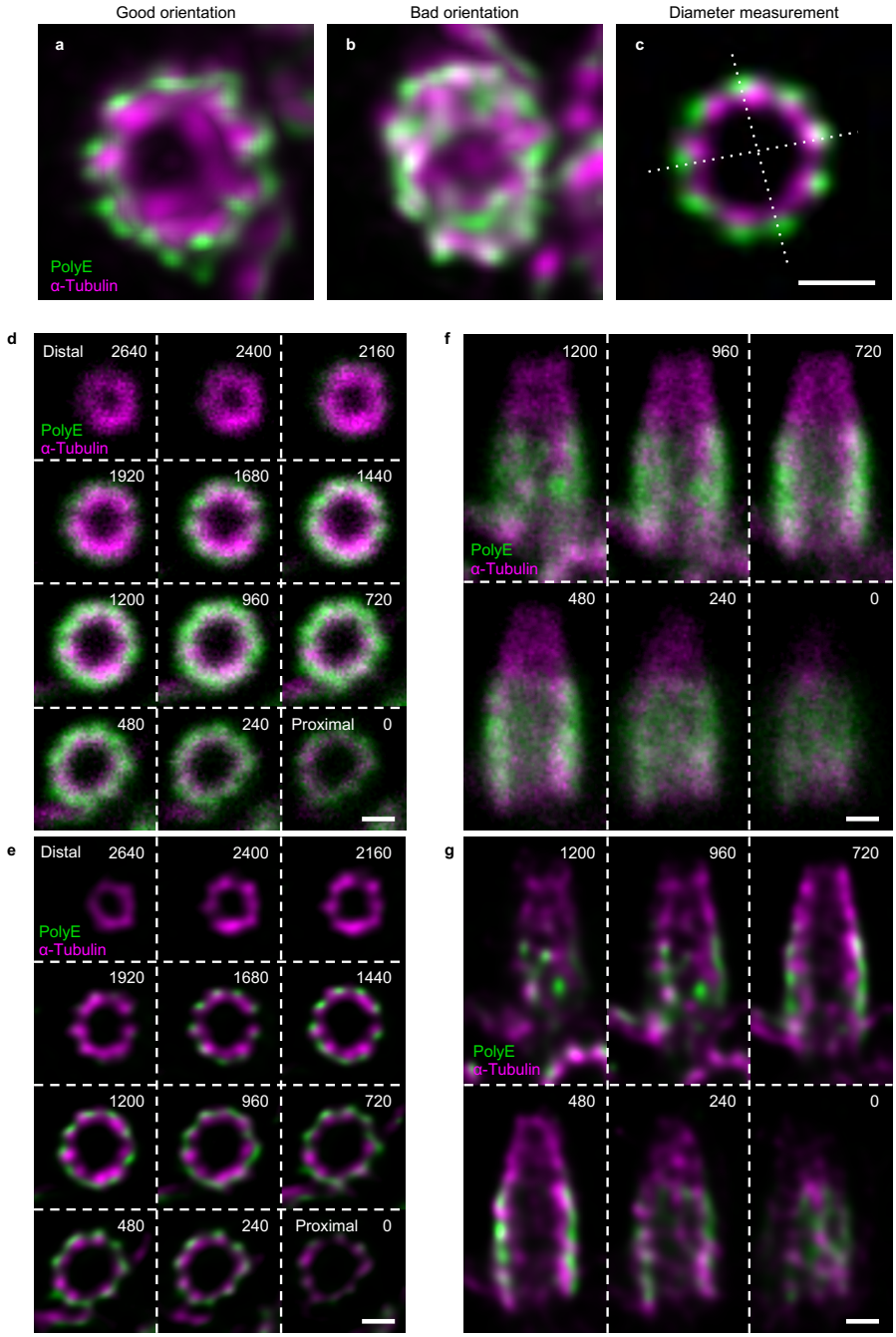

Supplementary Figure 2. Centriole diameter and length measurements. (**a**, **b**) Maximum intensity projection of a 3D image of an U-ExM *Chlamydomonas* centriole stained with tubulin (magenta) and PolyE (green) to illustrate a top view centriole in a good orientation (**a**) or a tilted orientation (**b**). Note that we excluded from our measurements tilted centrioles. (**c**) Illustration of centriole diameter measurement. Dotted lines represent the lines used to perform the measurements in Image J. An average of the two values was taken as the final diameter. Scale bar: 400nm. **(d, e)** Top view 3D image of an U-ExM *Chlamydomonas* centriole stained with tubulin (magenta) and PolyE (green) taken with confocal (**d**) or after Hyvolution (**e**). Steps every 240nm. Scale bar: 400nm. (**f**, **g**) Lateral view 3D image of an U-ExM *Chlamydomonas* centriole stained with tubulin (magenta) and PolyE (green) taken with confocal (**f**) or after Hyvolution (**g**). Steps every 240 nm. Scale bar: 400nm. Representative images from 3 independent experiments.

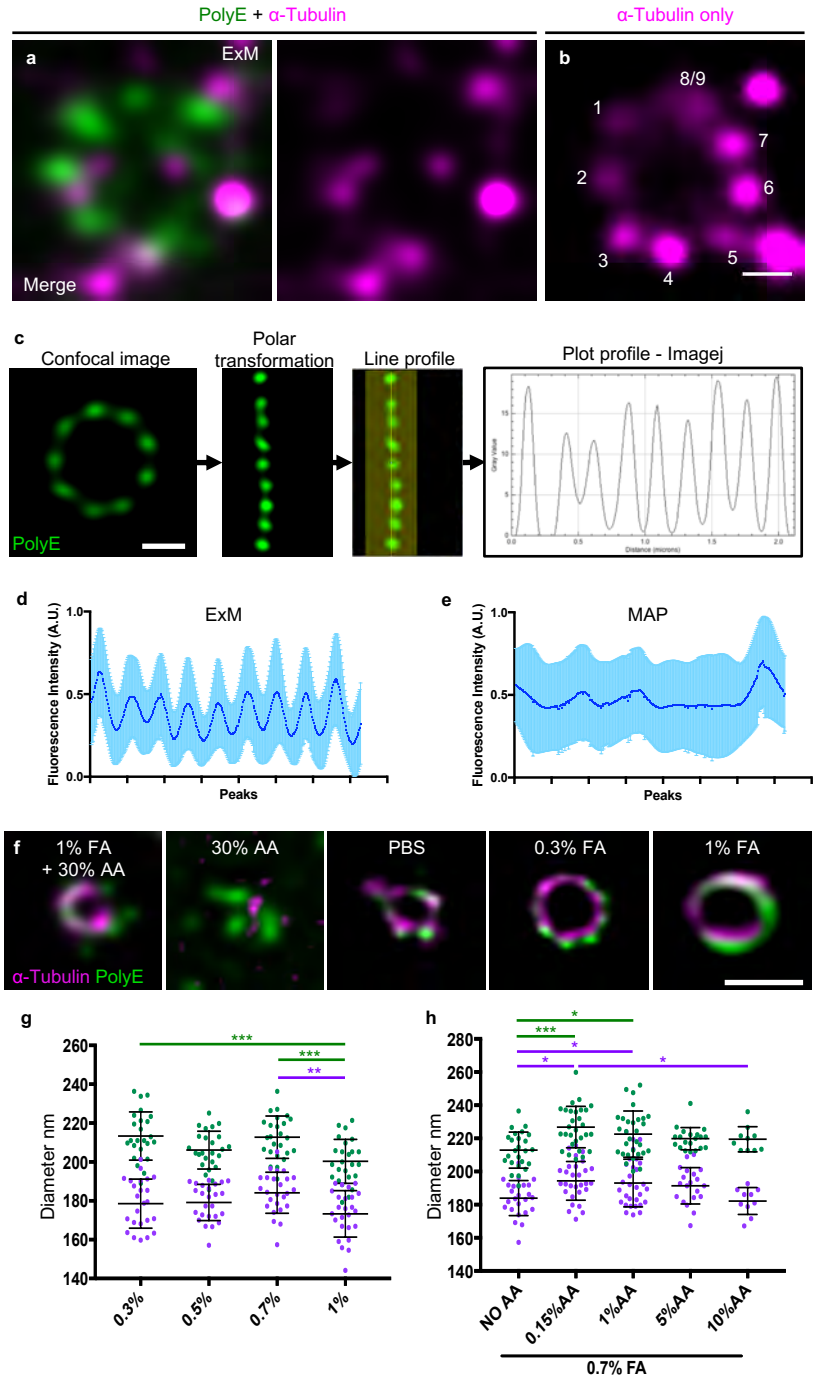

Supplementary Figure 3. Expansion conditions. (**a-b**) Representative confocal images (HyVolution) of isolated centrioles in ExM stained with PolyE (green, Alexa 568) and α-tubulin (magenta, Alexa 488) (**a**) or only α-tubulin (magenta, Alexa 488) (**b**). Note the 9-fold symmetry visible with tubulin in absence of the PolyE staining. Representative images from 3 independent experiments (**a**) and 1 experiment (**b**). Scale bar: 400nm. (**c**) Steps explaining how the 9-fold symmetry was analyzed starting from the confocal image to the polar transformation and the actual plot profile. Scale bar: 400nm. (**d**, **e**) Plot profiles of the polar transform showing the 9-fold symmetry for ExM (**d**) and MAP (**e**). The center line represents the average and the shaded region the standard deviation. n= 30 centrioles for each condition. Data from 3 independent experiments. (**f**) Representative confocal images (deconvolved by HyVolution) of isolated *Chlamydomonas* centrioles incubated in the reported

solutions before expansion in a MAP gel and stained with PolyE (green, Alexa 488) and α-tubulin (magenta, Alexa 568). Representative images from 2 experiments. Scale bar: 800nm. (**g**) Quantification of PolyE (green) and α-tubulin (purple) diameters of isolated *Chlamydomonas* centrioles incubated in the reported FA solutions. Average and standard deviation are as follows. PolyE: 0.3%: 213nm +/- 12; 0.5%: 206nm +/- 10; 0.7%: 213nm +/- 11 and 1%: 200nm +/- 11. Tubulin: 0.3%: 179nm +/- 13; 0.5%: 179nm +/- 9; 0.7%: 184nm +/- 11 and 1%: 173nm +/- 12. N=25 centrioles for each condition from 2 independent experiments. Statistical significance was assessed by ordinary one-way ANOVA test. Only statistically significant differences are shown: ***=0.0004 for 0.3% vs 1% and 0.0008 for 0.7% vs 1%. **=0.0049. (**h**) Quantification of PolyE (green) and α-tubulin (purple) diameters of isolated *Chlamydomonas* centrioles incubated in 0.7%FA without AA or in 0.7%FA + different concentration of AA (as reported in the graph). Average and standard deviation are as follows. PolyE: NO AA: 213nm +/- 11; 0.15% AA: 227nm +/- 12; 1%AA: 222nm +/- 14, 5%AA: 220nm +/- 7 and 10%AA: 219nm +/- 8. Tubulin: NO AA: 184nm +/- 11; 0.15% AA: 195nm +/- 12; 1%AA: 193nm +/- 14, 5%AA: 192nm +/- 11 and 10%AA: 182nm +/- 8. Data in condition NO AA are the same used in (**g**) as 0.7%. N=30 centrioles for conditions 0.15% AA and 1% AA from 3 independent experiments. For condition 0.7%FA + 5% AA, n=20 centrioles from 2 experiments and for condition 0.7%FA + 10% AA, n=10 centrioles from 1 experiment. Statistical significance was assessed by ordinary one-way ANOVA test. Only statistically significant differences are shown: *=0.018 for PolyE in NO AA vs 1% AA, 0.014 for Tubulin in NO AA vs 0.15% AA, 0.044 for Tubulin in NO AA vs 1% AA, and 0.046 for Tubulin in 0.15% AA vs 10% AA. ***=0.0002.

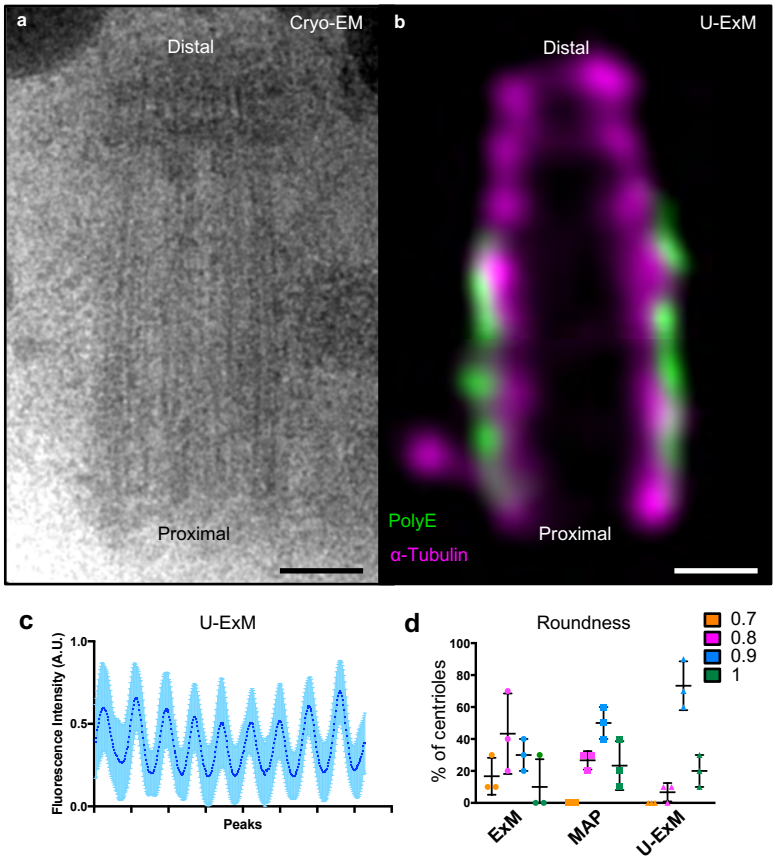

Supplementary Figure 4. U-ExM preserves the ultrastructure of centrioles. (**a**) Cryo-electron microscopy image representing a lateral view of an isolated *Chlamydomonas* centriole. (**b**) Same confocal image (deconvolved by HyVolution) shown in **Fig. 1d** of an isolated centriole expanded with U-ExM (0.7%+ 1% AA) and stained with PolyE (green, Alexa 488) and α-tubulin (magenta, Alexa 568). Representative lateral view from 3 independent experiments. Scale bars in (**a**): 100nm and (**b**): 400nm. (**c**) Plot profile of the polar transform showing the 9-fold symmetry for U-ExM. The center line represents the average and the shaded region the standard deviation. n= 30 centrioles. Data from 3 independent experiments. (**d**) Roundness, shape of the centriole for the three expansion methods. Averages and standard deviation are as follows. For ExM: 0.7=16.67 ± 11.55, 0.8= 43.33 ± 25.17, 0.9=30 ± 10, 1=10 ± 17.32. For MAP, 0.7=0 ± 0, 0.8=26.67 ± 5.77, 0.9= 50 ± 10, 1=23.33 ± 15.28. For U-ExM: 0.7=0 ± 0, 0.8=6.67 ± 5.77, 0.9=73.33 ± 15.28, 1=20 ± 10. Note that for all the quantifications provided in this figure, we included data from U-ExM performed with (0.7%FA + 0.15%) and (0.7%FA + 1% AA). N= 30 centrioles for each condition. Data from 3 independent experiments.

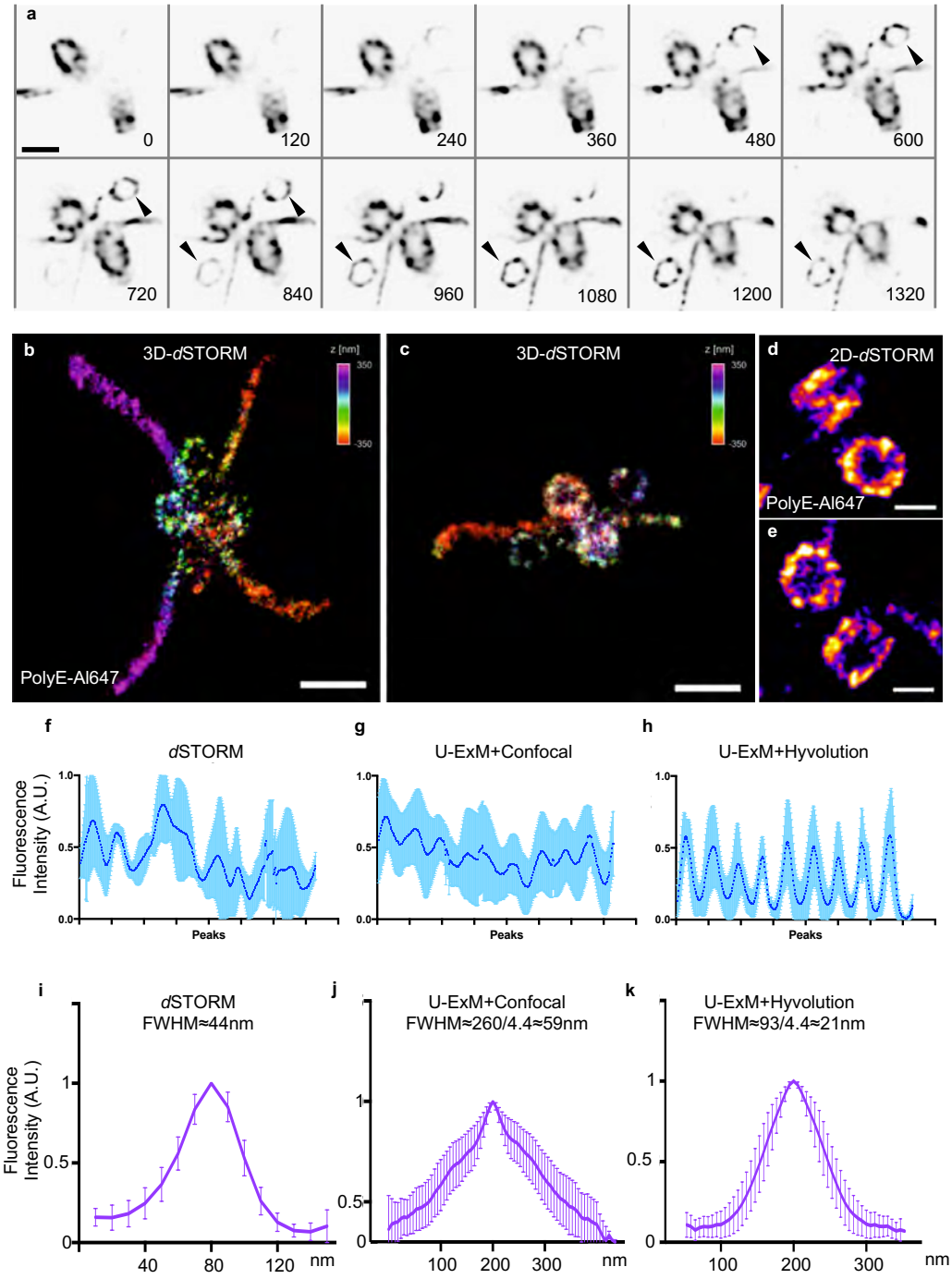

Supplementary Figure 5. Comparison of U-ExM to *d*STORM. (**a**) Montage of a Z-stack through *Chlamydomonas reinhardtii* isolated centrioles. Note the presence of procentrioles highlighted with the black arrowheads. Representative images from 3 independent experiments. (**b**, **c**) Examples of 3D projections of isolated centrioles fixed in FA and stained for PolyE using Al647. Imaging was performed using *d*STORM in 3D mode using a water objective. Representative images from 1 experiment. Scale bar: 500nm. (**d, e**) Two examples of isolated *Chlamydomonas* centrioles imaged using 2D *d*STORM with a oil objective. Representative images from 1 experiment. Scale bar: 200nm. (**f-h**) Plot profile of the polar transformation calculated from 2D-*d*STORM images of non-expanded procentrioles (**f,** n=4 procentrioles from one experiment), from confocal images of procentrioles expanded

with U-ExM (**g,** 30 precentrioles from 3 independent experiments) and from deconvoled images of the same procentrioles used in (**g**) using HyVolution (**h**, 30 precentrioles from 3 independent experiments). The center line represents the average and the shaded region, the standard errors. (**i-k**) Plot profile of the full width at half maximum (FWHM) calculated from procentrioles triplets: *d*STORM≈ 44nm (n=4 procentrioles, and 24 triplets from one experiment), U-ExM (confocal)≈ 59nm (n=9 procentrioles, and 76 triplets from 3 independent experiments), U-ExM (HyVolution)≈ 21nm (n=9 procentrioles, and 81 triplets from 3 independent experiments). Line connects the mean of each x value and error bars represent the standard deviation.

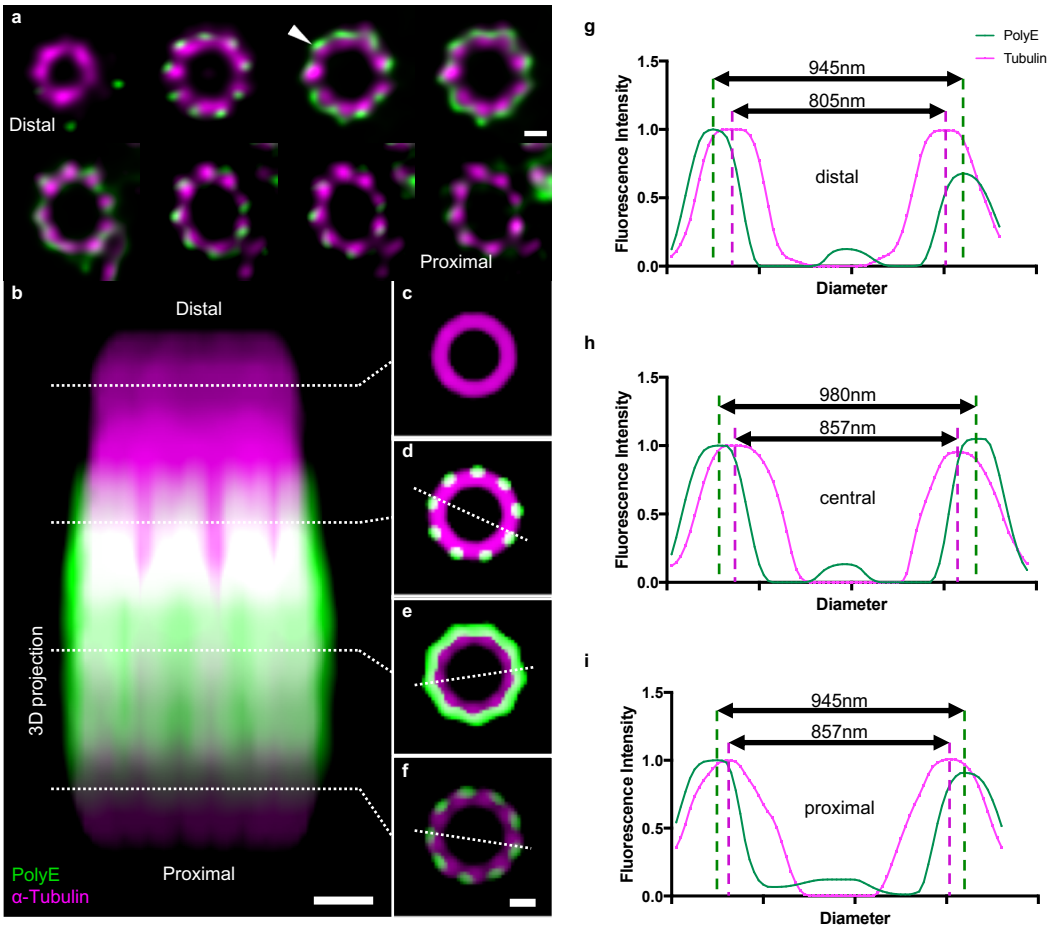

Supplementary Figure 6. Polyglutamylated tubulin localization in an isotropic reconstruction of a U-ExM centriole. (**a**) Gallery of a Z stack from distal to proximal of a mature centriole expanded using U-ExM (0.7%FA+1%AA) and stained with α-tubulin (magenta, Alexa568) and PolyE (green, Alexa488). Scale bar: 200nm. Arrowhead points to PolyE surrounding the tubulin signal. Representative data from 3 independent experiments. (**b**) 3D volume reconstruction of a mature *Chlamydomonas* centriole stained with α-tubulin (magenta, Alexa568) and PolyE (green, Alexa488). Scale bar: 200nm. Data obtained from 14 centrioles averaged (one experiment). (**c-f**) Sections through the centriole spanning the distal (**c**) and the central core (**d-f**) regions. Scale bar: 200 nm. (**g-i**) Quantification of PolyE and α-tubulin diameter for the distal (**g**), central (**h**) and proximal parts of the central core region of centrioles (**i**) corresponding to (**d**), (**e**) and (**f**), respectively. Data obtained from 14 centrioles averaged (one experiment). Note that the polyglutamylation diameter signal is larger than that of tubulin.

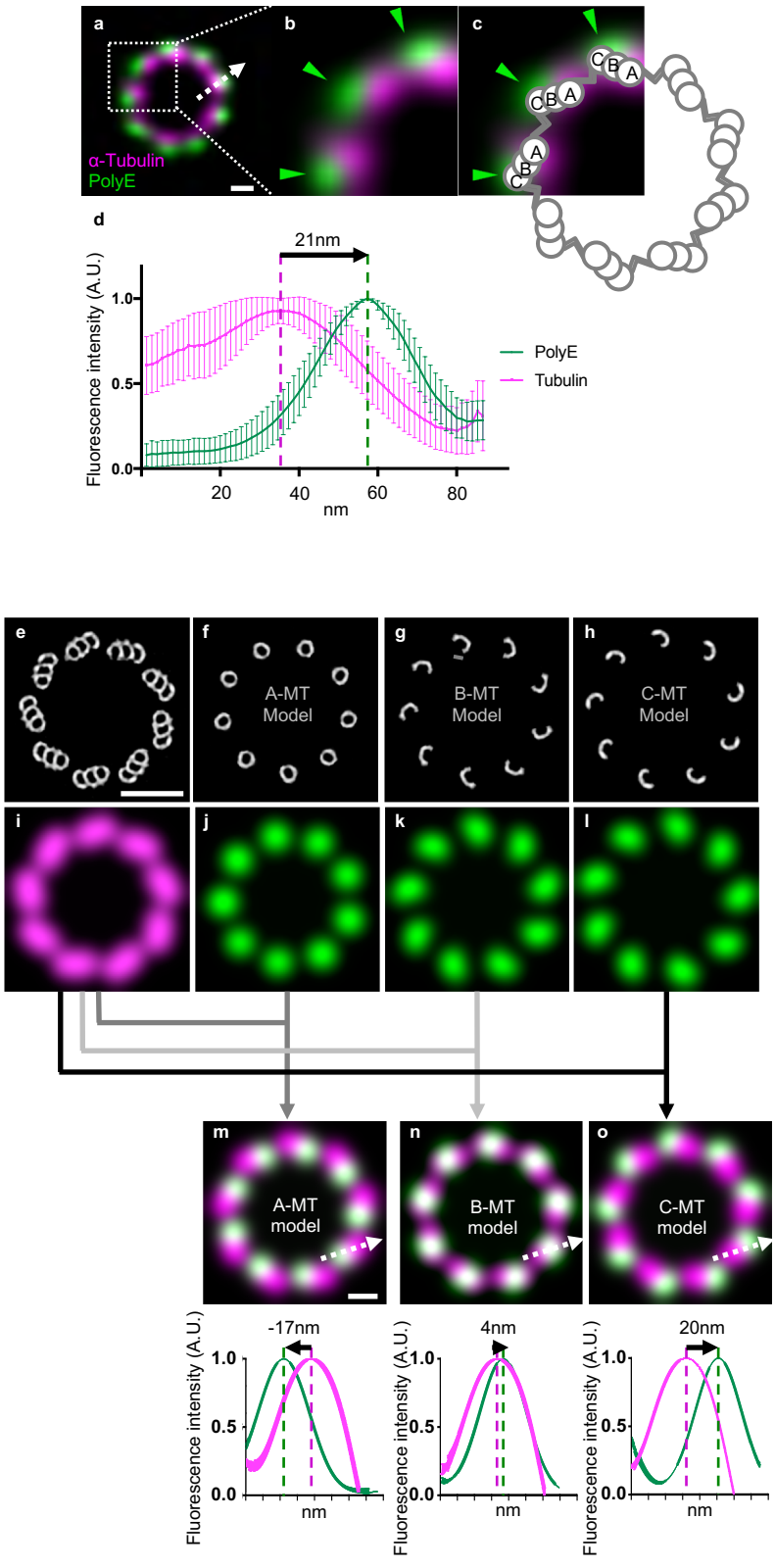

Supplementary Figure 7. PolyE sub-triplet localization revealed by U-ExM. (a-c) Representative image taken from a Z-stack of the distal most-part of the central core of a deconvolved mature centriole stained for α-tubulin (magenta, Alexa568) and PolyE (green, Alexa488). Scale bar: 200nm. Green arrowheads highlight the PolyE signal (**b, c**). The dotted arrow in (**a**) illustrates how the fluorescence intensity was measured in **(d)**. (**c**) Schematic representation of microtubule triplets superimposed

onto the fluorescent signal shown in **b**. (**d**) Quantification of the fluorescence intensity shift between the magenta and the green signal. Note that the shift is of 21 nm (n=61 triplets from 8 centrioles). Data from 3 independent experiments. Line connects the mean of each x value and error bars represent the standard deviation. (**e-h**) Model images of a *Chlamydomonas* centriole with entire triplets (**e**) only A-tubule (**f**) only B-tubule (**g**) and only C-microtubule (**h**). Images were scaled to mimic an expanded centriole. Scale bar: 500 nm. (**i-l**) Images were bandpass filtered to obtain a resolution of 140 nm typical of a confocal microscope in HyVolution mode. Colors are added to mimick fluorescent signal. (**m-o**) Model representation of PolyE signal onto specific microtubule blades, A- (**m**), B- (**n**) and C- (**o**). Note that in this model, the entire triplet is stained with α-tubulin (magenta). Below is represented the fluorescence peak shift between the two colors in each condition. Scale bar: 200nm.

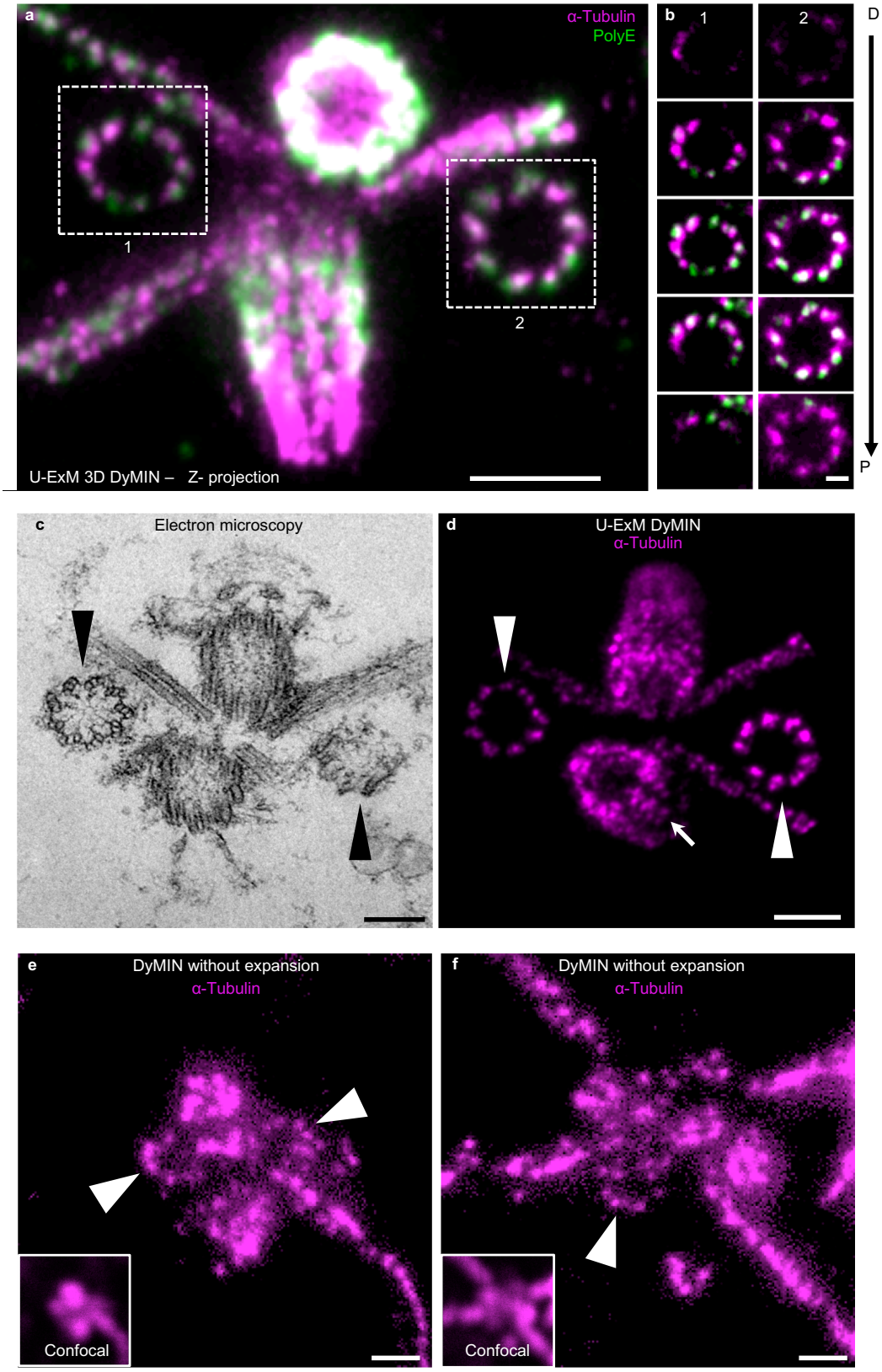

Supplementary Figure 8. Coupling STED to U-ExM. (**a**) 3D DyMIN images of U-ExM (0.7% FA+1% AA)-treated centrioles stained with PolyE (green, STAR 580) and α-tubulin (magenta, STAR RED). Maximum intensity projection. Data from one experiment. (**b**) Stack slices thought the procentrioles. Scale bar in (**a**): 1µm, (**b**): 200nm. (**c**) Electron microscopy (EM) image of a centriole pair comprising two

mature centrioles and two procentrioles (black arrowheads) interconnected by striated fibers. Scale bar: 200nm (**d**) A similar centriole pair stained for α-tubulin (magenta, STAR RED) after U-ExM (1% FA) and imaged using DyMIN. Note that the overall ultrastructure of this organelle resembles the EM image. White arrowheads points to procentrioles and the arrow points to the mature centriole. Data from 2 independent experiments. Scale bar: 800nm.
(**e, f**) Two representative DyMIN images of non-expanded *Chlamydomonas* isolated centrioles stained for α–tubulin (magenta). Insets show the same centriole imaged at confocal. White arrowheads indicate procentrioles. Data from one experiment. Scale bar: 200nm.

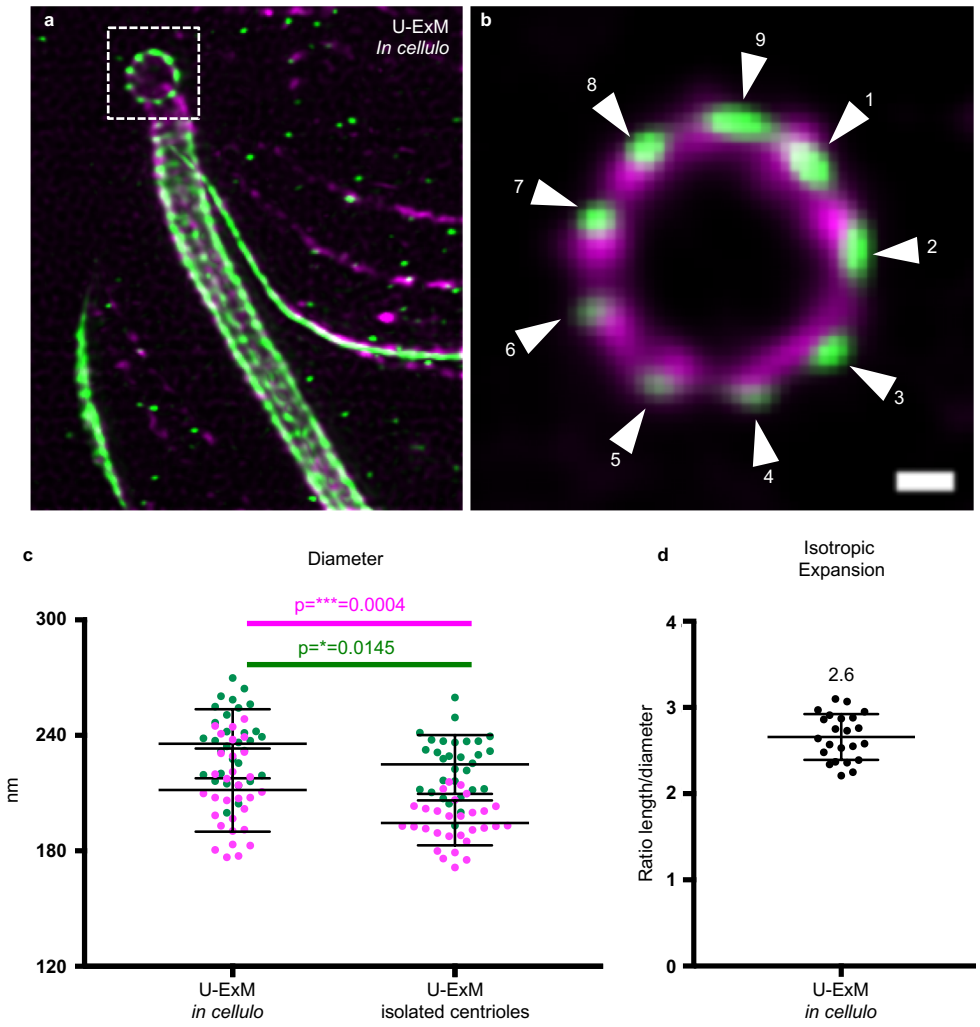

Supplementary Figure 9. *In cellulo* expanded *Chlamydomonas* centrioles. (**a**, **b**) Representative Hyvolution confocal image of an *in cellulo Chlamydomonas* centriole stained for PolyE (green) and α–tubulin (magenta). The dotted square highlight the centriole shown in the inset (**b**). Arrowheads indicate the nine-fold symmetry of the centriole. Scale bar: 250nm. Representative images from 3 independent experiments. (**c**) Diameter in nm of U-ExM centrioles *in cellulo* or from purified centrioles. Averages and standard deviation are as follows. PolyE: 236 nm +/-18 nm for U-ExM *in cellulo* (n=31 centrioles) and 225 nm +/- 15 nm for U-ExM isolated centrioles (n=30 centrioles). α-tubulin: 212 nm +/- 22 nm for U-ExM *in cellulo* (n=31 centrioles) and 195 nm +/- 12 nm for U-ExM isolated centrioles (n=29 centrioles). Data from 3 independent experiments. Note that centrioles *in cellulo* are statistically slightly larger. Unpaired two-sided t-test: for PolyE: p= 0.0145 and tubulin: p= 0.0004. (**d**) Isotropic expansion calculated by the ratio of centriolar length/diameter. Average and standard deviation are as follows: 2.6 +/- 0.3 (n=23 centrioles from 3 independent experiments). Unpaired two-sided t-test = 0.68 (non significative) compared to U-ExM isolated centrioles (**Fig. 1f**). Note that centrioles *in cellulo* expanded isotropically.

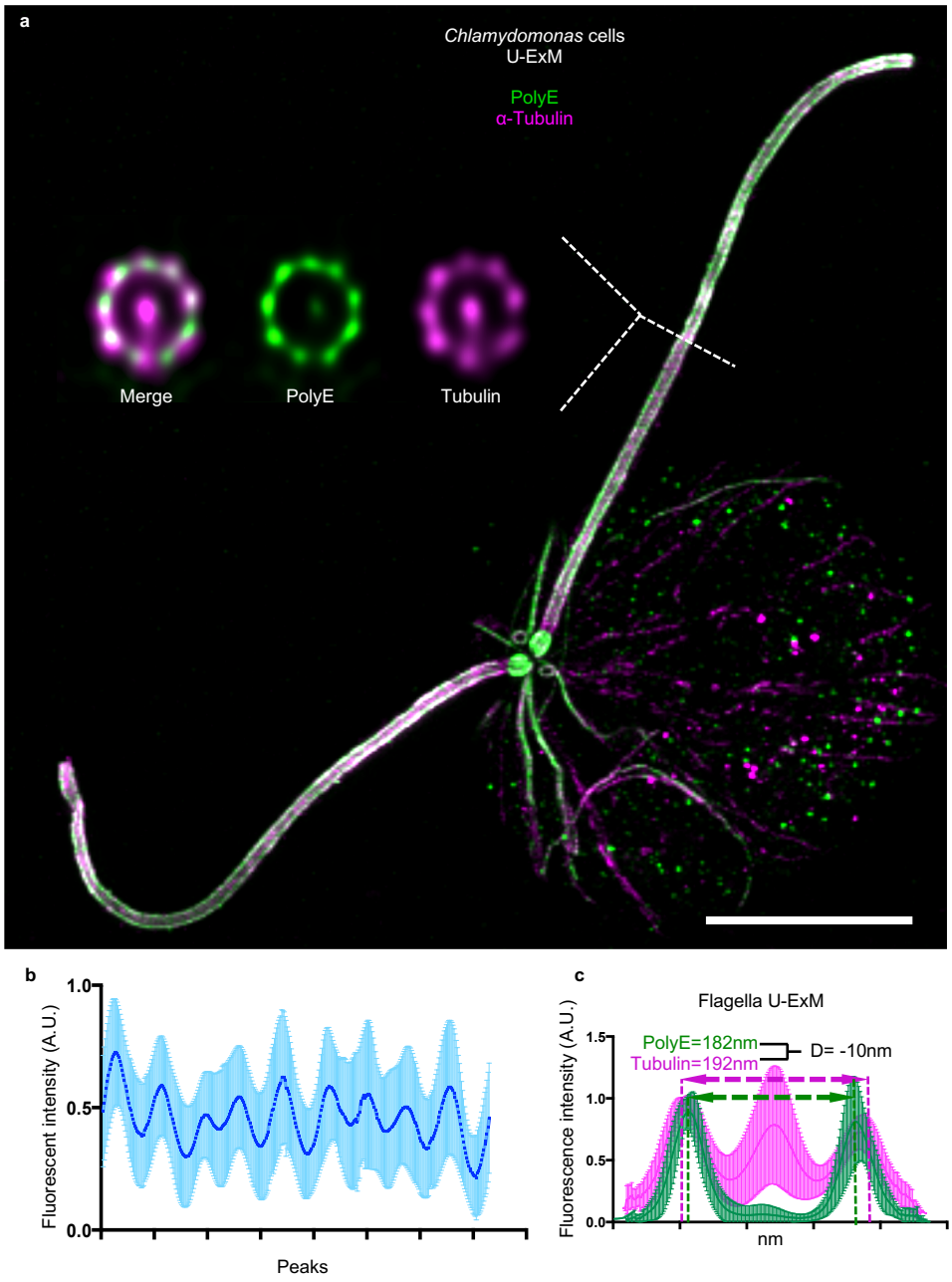

Supplementary Figure 10. U-ExM applied on *Chlamydomonas* cells. (a) *In cellulo* U-ExM expansion of a *Chlamydomonas* cell stained with PolyE (green) and α–tubulin (magenta) imaged using confocal microscopy coupled to Hyvolution. Scale bar: 13µm. Representative image of a top-view across a flagellum. Note that the nine doublets are highly polyglutamylated (green) while the central pair is weakly polyglutamylated. Representative images from 3 independent experiments. (**b**) Plot profile of the polar transform showing the 9-fold symmetry of the axoneme. The center line represents the average and the shaded region, the standard errors. N=23 axoneme from 3 independent experiments. (**c**) Quantification of the fluorescence intensity shift between the magenta and the green signal showing that the PolyE signal is more internal than the tubulin signal with a shift of -10 nm. Line connects the mean of each x value and error bars represent the standard deviation. N= 23 axonemes from 3 independent experiments.

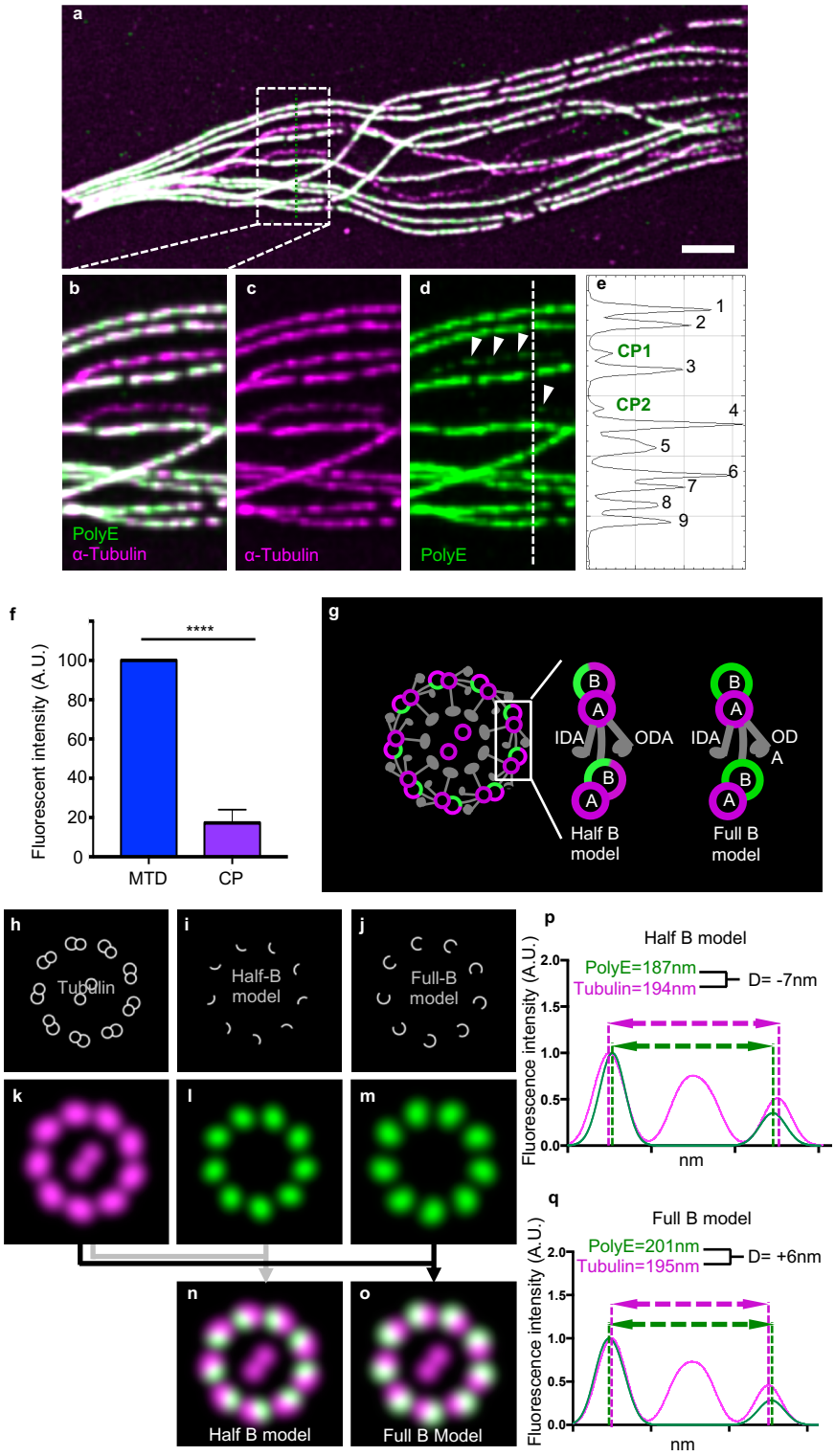

Supplementary Figure 11. Analysis of the Polyglutamylation profile in axonemes using U-ExM. (**a-d**) Opened axoneme stained with PolyE (green, Alexa 488) and α-tubulin (magenta, Alexa 568). (**b-d**) Inset of the region boxed in (**a**). Scale bar: 1µm. (**e**) Plot profile of the PolyE signal over the 9 microtubule doublets and the 2 central

pairs. Numbers represent single microtubules doublets (MTD) while CP1 and CP2 are individualized microtubules of the central pair. Representative images and plot profile from one experiment (n=4 sprayed flagella). (**f**) Fluorescence intensity (A.U) of MTD and CP. Note that CPs display a weak PolyE signal. Average and standard deviation is as follows: Average intensity of CP= 17% +/- 7 unpaired t test two-tailed, $p< 0.0001$. Data from one experiment (n= 4 sprayed flagella). (**g**) Schematic representation of an axoneme composed of nine outer microtubule doublets and a central pair of single microtubules (9+2). Microtubules are in magenta; inner dynein arms (IDA), outer dynein arm (ODA), nexin and radial spokes are in grey; polyglutamylated tubulin is in green. Note that we draw two models: one with polyglutamylated tubulin restricted to the inner side of the B-tubule (half B) and one with the entire B-tubule decorated (Full B). (**h-j**) Model images of a *Chlamydomonas* flagellum adapted from a cryoEM map with the entire microtubule doublets (**h**), only half B-tubule (**i**) and only full B-tubule (**j**). Images were scaled to mimic an expanded axoneme. (**k-m**) Bandpass filtered images to obtain a resolution of 140 nm typical of a confocal microscope in HyVolution mode. Colors are added to mimics fluorescent signal. (**n-o**) Model combining the α-tubulin and PolyE signals to show how the PolyE signal in either half B-microtubule or full B-microtubule would be positioned in relation to the α-tubulin signal of the entire doublet. (**p**, **q**) Fluorescent peak shift between the magenta and the green signal for the Half B (**p**) and the Full B (**q**) models. The shifts are -7 nm and +6 nm, respectively. Note that the experimental data mimics the Half B model (**p**).

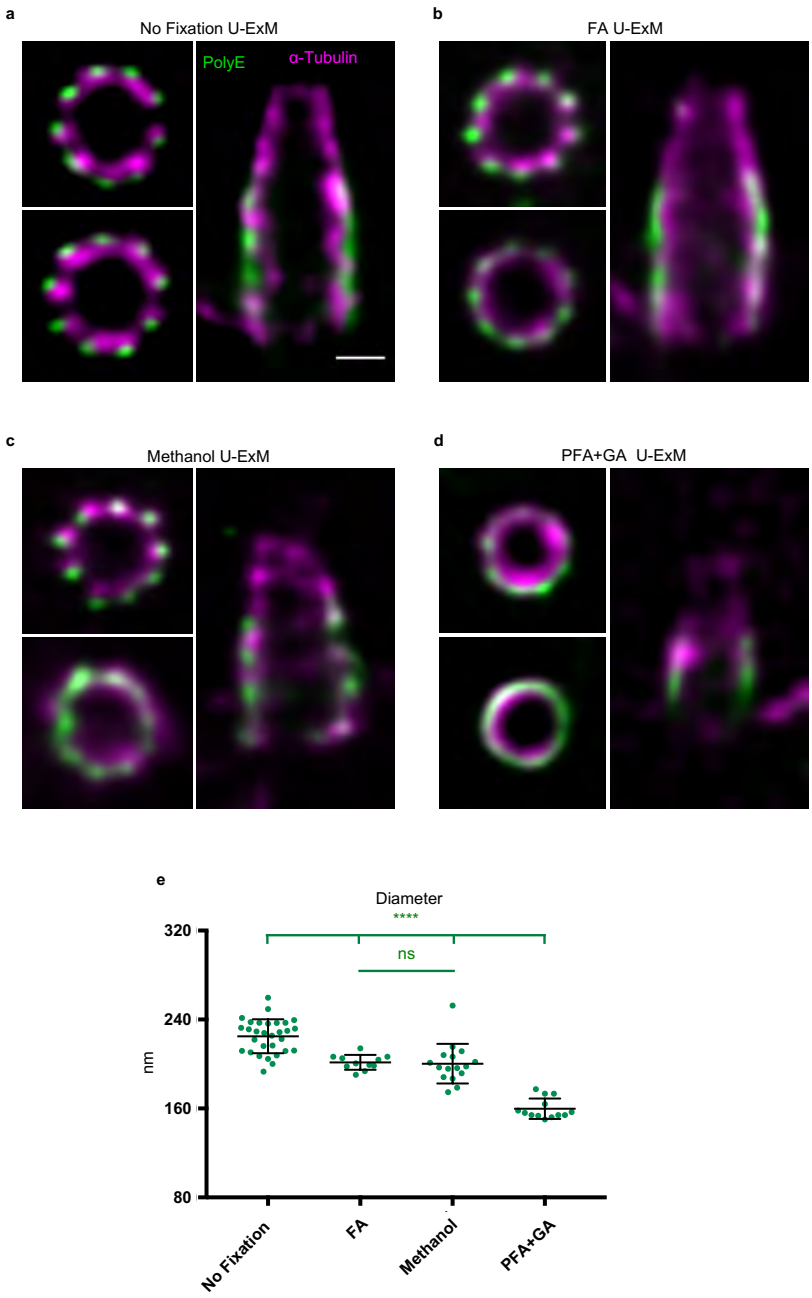

Supplementary Figure 12. Effect of different fixations on U-ExM-isolated *Chlamydomonas* centrioles. (**a-d**) 2 examples of top (left) and one example of lateral (right) views of Hyvolution images of centrioles unfixed (**a**) or fixed with FA (**b**), methanol (**c**) or PFA/GA (**d**) stained with α-tubulin (magenta) and PolyE (green). Scale bar: 400nm. (**e**) Diameter of the centrioles in the indicated conditions. Averages of PolyE diameter and standard deviations are as follows: no fixation: 225 nm +/- 15 nm; FA: 201 nm +/- 7 nm (n=11); methanol: 200 nm +/- 18 nm (n=16); PFA/FA: 160 nm +/- 9 nm (n=13). For 'No fixation' condition, same data from **Fig. 1e** was used. For methanol fixed condition, data from 2 independent experiments. For FA and PFA/GA conditions, data from 1 experiment. Statistical significance was assessed by one-way ANOVA test: ****<0.0001, ns (non significant)=0.996.

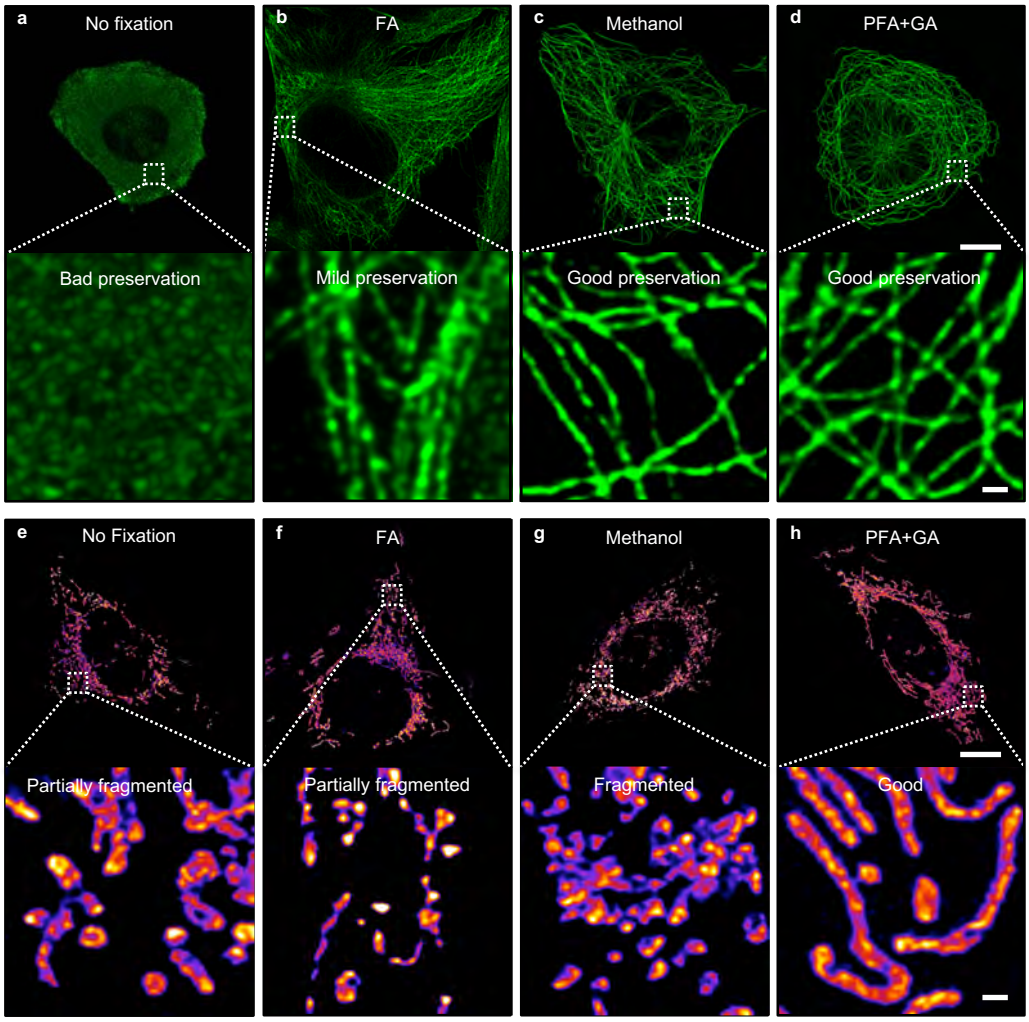

Supplementary Figure 13. Effect of different fixations on cellular structures in human cells. (**a-d**) Representative Hyvolution images (from 2 independent experiments) of U2OS cells unfixed (**a**) or fixed with FA (**b**), methanol (**c**) or PFA+GA (**d**) and stained with α-tubulin (green). Scale bar: 10µm. Insets (shown with the dotted square) show a magnified region. Scale bar: 0.5µm. (**e-h**) Representative Hyvolution images (from 2 independent experiments) of U2OS cells unfixed (**e**) or fixed with FA (**f**), methanol (**g**) or PFA+GA (**h**) and stained with mitotracker (fire). Scale bar: 10µm . Insets (shown with the dotted square) show a magnified region. Scale of insets: 500nm. Note that only PFA/GA preserves the mitochondrial organization.

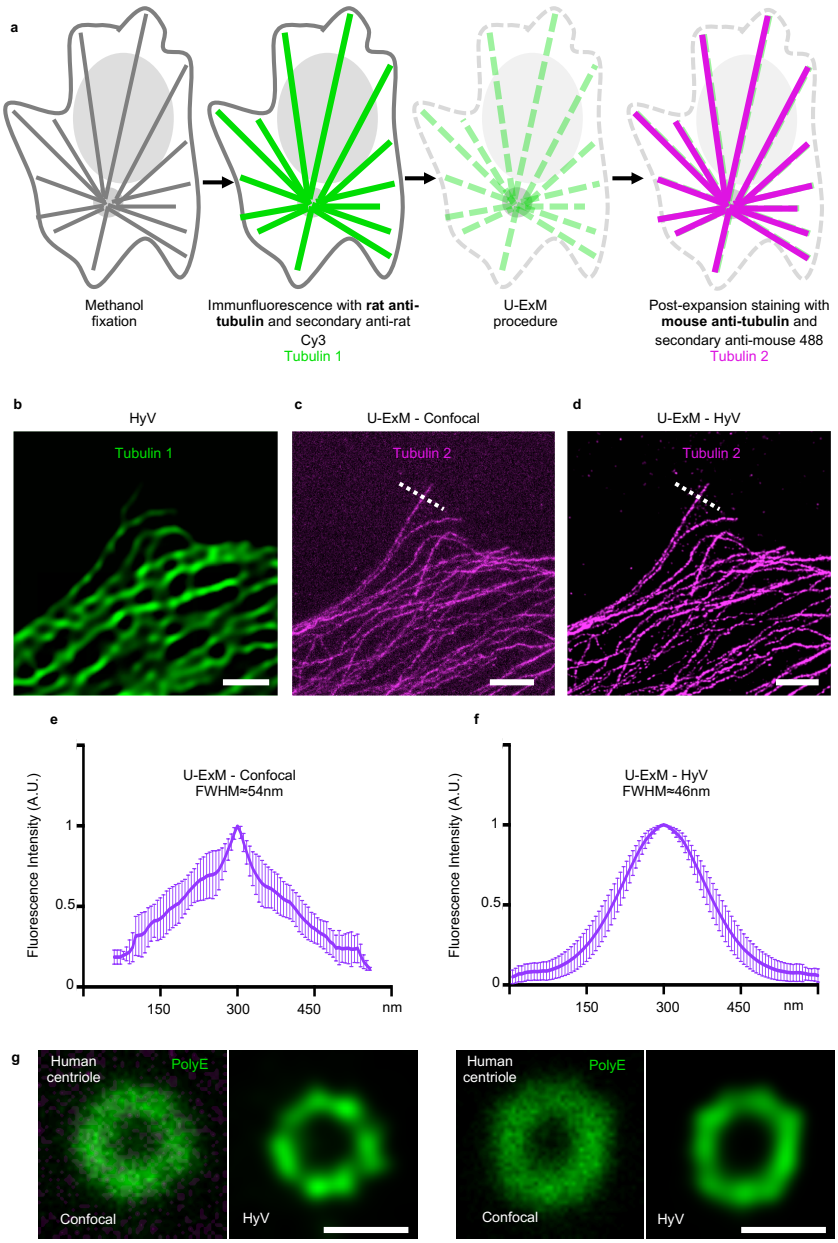

Supplementary Figure 14. U-ExM applied on human cells. (**a**) Schematic illustration of the pre and post-U-ExM expansion imaging experiment. U2OS cells were first methanol fixed and immonostained with a rat anti-tubulin (tubulin 1, green) followed by imaging. Then, cells were processed for U-ExM. Post staining was performed with mouse anti-tubulin (tubulin 2, magenta). (**b-d**) Inset of a U-ExM-U2OS cell processed for pre- (**b**) and post expansion imaging (**c**, confocal; **d**, Hyvolution) as depicted in (**a**). Scale bars: 1.5µm (**a**) and 6 µm (**c**, **d**). Representative images from 1 experiment, n=4 cells. (**e**, **f**) Plot profiles of the regions indicated with a dotted white line with the corresponding full width at half maximum (FWHM): confocal, U-ExM microtubule: 54 nm (n=47); Hyvolution, U-ExM microtubule: 46 nm (n=50). Line connects the mean of each x value and error bars represent the standard deviation. Data from 3 independent experiments. (**g**) Two examples of human centrioles expanded using U-ExM in cells and imaged at confocal (left) or Hyvolution (right). Data from one experiment. Scale bar: 800nm.

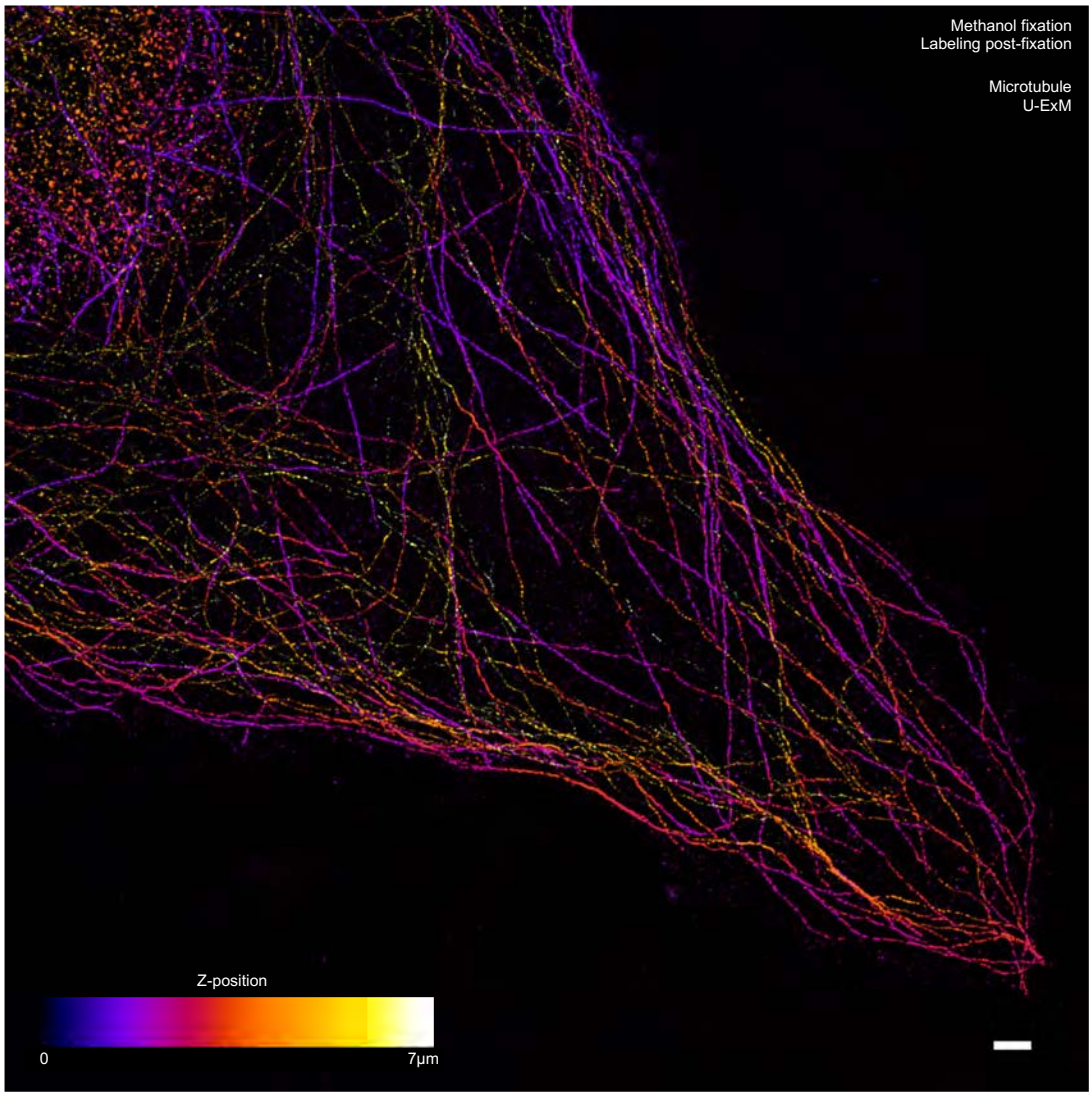

Supplementary Figure 15. U-ExM microtubules. Hyvolution image of microtubules from a U2OS cell fixed with methanol and processed for U-ExM. Color code indicates the Z-position . Representative images from 3 independent experiments. Scale bar: 4µm.

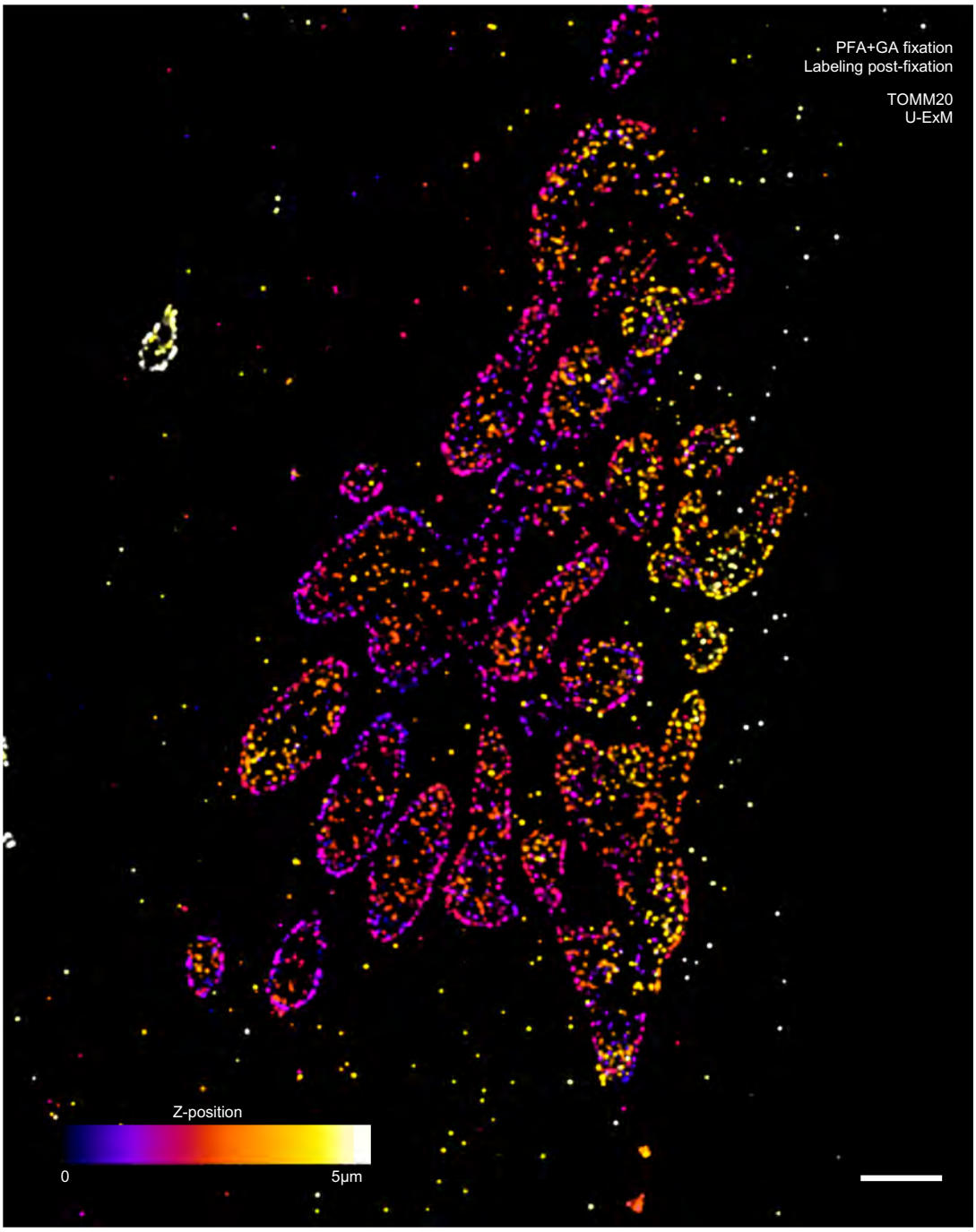

Supplementary Figure 16. U-ExM mitochondria. Hyvolution image of mitochondria from a U2OS cell fixed with PFA/GA, processed for U-ExM and stained for the outer membrane mitochondrial translocase TOMM20. Color code indicates the Z-position. Representative images from 3 independent experiments. Scale bar: 4µm.

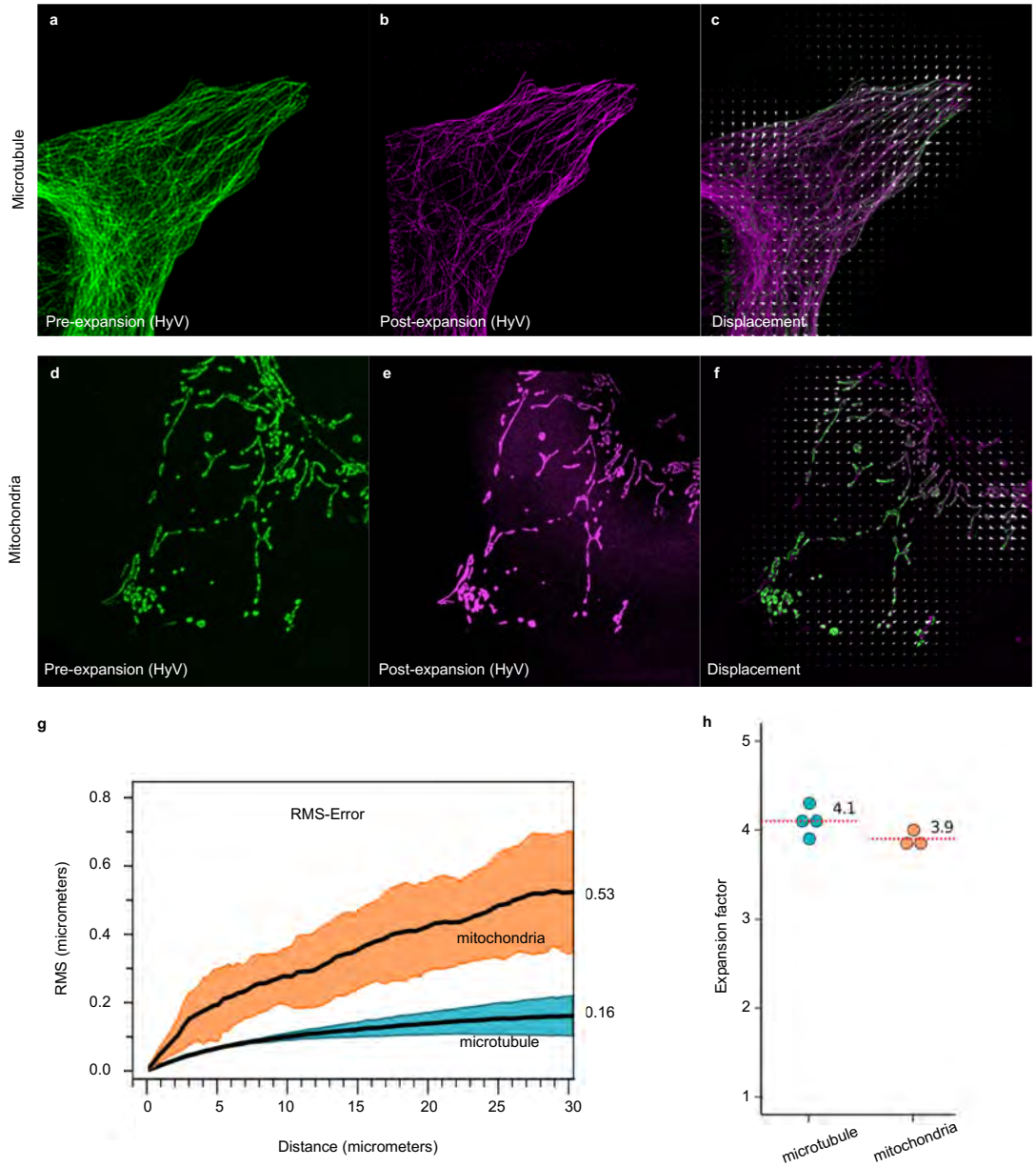

Supplementary Figure 17. Evaluation of distortions over length scales for microtubules and mitochondria staining. (**a**, **b**) Hyvolution images of a U2OS cell treated for pre- (**a**) (tubulin 1, green) and post-expansion imaging (tubulin 2, magenta) (**b**). (**c**) Overlay of pre- and post- expansion images of microtubules with distortion vector field. Representative images from 1 experiment. (**d**, **e**) Hyvolution images of a U2OS cell treated for pre- (**d**) (mitotracker 1, green) and post-expansion imaging (mitotracker 2, magenta) (**e**). (**f**) Overlay of pre- and post- expansion images of mitochondria with distortion vector field. Representative images from 2 experiments. (**g**) Quantification of root mean square (RMS) error over distance (micrometers) comparing pre- (**a, d**) and post-U-ExM (**b, e**) expansion for both microtubules (n=4 cells from 1 experiment) and mitochondria (n=3 cells from 2 experiments). Line connects the mean of each x value and error bars represent the standard deviation. (**h**) Calculated expansion factor based on the RMS graph for both microtubules (n=4 cells from 1 experiment) and mitochondria (n=3 cells from 2 experiments). Red dotted lines correspond to the averages: 4.1 for microtubules and 3.9 for mitochondria.

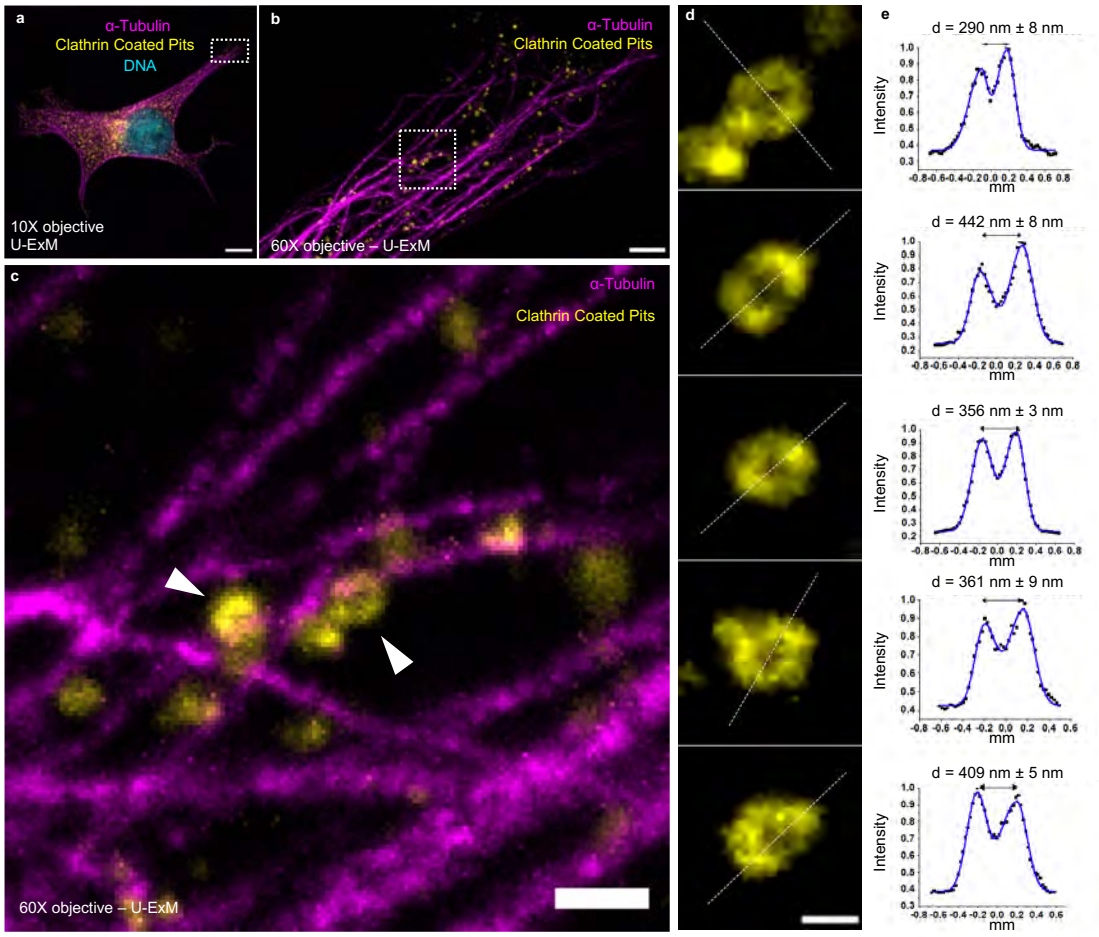

Supplementary Figure 18. Clathrin Coated Pits visualized after U-ExM.
(**a**) Representative image of a human cell stained for tubulin (magenta), clathrin coated pits (yellow) and DNA (blue) with a 10x objective. Scale bar: 40µm. Data from 3 independent experiments. (**b**) Same cell imaged with a 60X objective highlighting the clathrin coated pits. Scale bar: 4µm. (**c**) Zoom in of the region shown with the squared dotted line. White arrowheads indicate clathrin-coated pits. Scale bars: 1µm. (**d**) Gallery of U-ExM clathrin-coated pits. Note the hollow shape of the clathrin pits. Scale bar: 400nm. (**e**) Plot profiles along the clathrin-coated pits, as indicated in (**d**) with a dotted line, highlighting the hollow center in the clathrin pits. Double gaussian fits (blue line) of the normalized intensity profiles were used to calculate the diameter of the pits with standard errors deriving from the fits. Using an expansion factor of 4x, the values translate to: 72nm, 110nm, 178nm, 90nm and 102nm.

Conditions	20%AA/7%SA	10%AA/7%SA	10%AA/19%SA	5%AA/7%SA	5%AA/19%SA
Expansion Factor	3.40 ± 0.08	3.60 ± 0.04	4.00 ± 0.02	3.90 ± 0.06	4.30 ± 0.0
Correct shape	✓	✓	✓✓ U-ExM	✗	✗

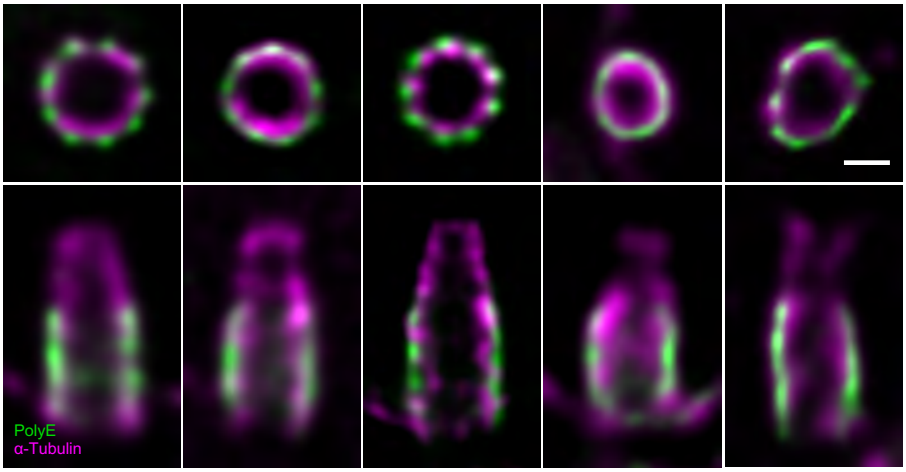

Supplementary Figure 19. Optimization of the U-ExM expansion factor. (Online Methods). Monomer solutions of different composition were tested for gel expansion. Averages expansion factor with their corresponding standard error of the mean are indicated (data from 2 independent experiments). Centriolar shape was analyzed: ✓ indicates proper shape and ✗ deformed centrioles. Below are representative top and side views from 2 independent experiments of Hyvolution-images of isolated *Chlamydomonas* centrioles treated in the indicated conditions. Centrioles were stained for tubulin (magenta) and PolyE (green). Scale bar: 450nm. Note that U-ExM gave the best structural preservation of the specimen.